AMERICAN UNIVERSITY OF BEIRUT

DEVELOPMENT OF AN ECO-FRIENDLY MASK FROM LOCAL PLANT BYPRODUCTS

by
AYOMIDE JACOB ADEOYE

A thesis
submitted in partial fulfillment of the requirements
for the degree of Master of Science
to the Biomedical Engineering Program
of Maroun Semaan Faculty of Engineering and Architecture
and the Faculty of Medicine
at the American University of Beirut

Beirut, Lebanon
September 2022

AMERICAN UNIVERSITY OF BEIRUT

DEVELOPMENT OF ECO-FRIENDLY FILTERS FROM LOCAL PLANT BYPRODUCTS

by
AYOMIDE JACOB ADEOYE

Approved by:

	Signature
Dr. Rami Mhanna, Assistant Professor Biomedical Engineering Program	Advisor
	Signature
Dr. Antoine Abou Fayad, Assistant Professor Faculty of Medicine	Co-Advisor
	Signature
Dr. Mohammad Harb, Assistant Professor Mechanical Engineering Program	Member of Committee
Walid Saad	Signature
Dr. Walid Saad, Associate Professor Chemical Engineering and Advanced Energy Program	Member of Committee

Date of thesis defense: September 05, 2022

AMERICAN UNIVERSITY OF BEIRUT

THESIS RELEASE FORM

Student Name: Adeoye_____Ayomide_____Jacob_____

I authorize the American University of Beirut, to: (a) reproduce hard or electronic copies of my thesis; (b) include such copies in the archives and digital repositories of the University; and (c) make freely available such copies to third parties for research or educational purposes:

- ☐ As of the date of submission
- ☒ One year from the date of submission of my thesis.
- ☐ Two years from the date of submission of my thesis.
- ☐ Three years from the date of submission of my thesis.

_____ September 8, 2022_____

Signature Date

ACKNOWLEDGEMENTS

According to the American University of Beirut (AUB) motto which states, “That they may have life and have it more abundantly”. I express my deepest and heart felt appreciation to Mastercard Foundation Scholar (MCF) program for giving me a life by funding my master's degree at AUB and for their moral support. Accolades to AUB for transforming me to a better person and for giving me life more abundantly.

I appreciate Dr. Rami Mhanna, my supervisor, for his support towards the successful completion of my thesis requirement. It has always been a great pleasure to have you as a course advisor, thesis supervisor and to take some courses taught by you. The drug delivery course and the thesis research opened the door to great opportunities for me.

I am grateful to my co-advisor, Dr. Antoine Abou Fayad, and the members of the committee, Dr. Mohammad S. Harb and Dr. Walid Saad, for their time, assistance, comments, and ideas that improved the research successfully. Through my supervisor, co-advisor, committee members, George Deeb and Malak El-Tfayli support, I was able to present my research at the 6th CRSL research conference at the American University of Beirut. I appreciate Dr. Mohammed Dakdouki from Beirut Arab University, who provided some materials used in this research.

I wish to express my heart felt appreciation to George Deeb (a PhD candidate in Dr. Rami’s lab) for accepting me as his student, brother, and mentee. He was supportive in terms of experimental analysis and expediting my request for chemicals by following up with Tala Bechara.

I am grateful to Tala Bechara for her support in terms of following up with AUB stores to supply chemicals I needed. I appreciate her for never getting tired of sending emails to make sure I get my order as soon as possible. My immense appreciation goes to the following people who have in one way or the other contributed to the success of my research; Rania Shatila, Nareg Karaoghlanian, Alissa Haissam, Jad Awad, Philip Adebayo, Akimana Godiolla, Miriam and Grace. To my great friends, MCF family and lab members, I appreciate your advice and support most especially during thesis adversity.

To my wonderful parents (Mr. and Mrs. Adeoye), siblings (Kayode Adeoye and Tunmise Adeoye) and Mr. Adeoya Adebayo, your unwavering love has been my rock and motivation. I am delighted to have you all in my life.

ABSTRACT
OF THE THESIS OF

Ayomide Jacob Adeoye for Master of Science
Major: Biomedical Engineering

Title: Development of Eco-Friendly Filters from Local Plant Byproducts

Filters used in face masks or in devices (such as HEPA filters) are essential tools against airborne pathogens such as severe acute respiratory syndrome coronavirus 2 (SARS-CoV-2 or Covid-19), and adsorbing hazardous gases. The various components of a face mask include an air filter, nose adapter, and elastic ear loops. Each component is constructed of different materials, such as polypropylene or polyester for the filter, aluminum for the nasal adapter, and elastane for the elastic loops. According to recent studies, over 129 billion face masks are used globally every month due to the Covid-19 pandemic. The manufacturing of masks and filters necessitates a large consumption of fossil-based materials and the generation of large amounts of toxic waste, both of which can result in environmental pollution, infection, and ozone layer depletion. The objective of this research is to contribute to environmental sustainability through extraction of cellulose from sugarcane bagasse (SCB) and banana midrib (BMR) by treating them (SCB and BMR) with ethanol and sodium hydroxide, followed by formic and acetic acid, then performic and peracetic acid, and finally hydrogen peroxide to fabricate eco-friendly filters. The resulting materials were purified to remove impurities (such as lignin and hemicellulose) and were then characterized using scanning electron microscope (SEM), universal testing machine (UTM), capillary flow porometer, condensation particle counter, and thermogravimetric-Fourier transform infrared spectroscopy (TG-FTIR) analysis after each treatment to assess fiber type, mechanical property, pore size, filtration efficiency, flow resistance, thermal properties and chemical composition. The SEM analysis showed the microstructure of the cellulose membrane extracted from SCB and BMR which varied from aggregated cellulose structures to a fibrous mesh depending on the treatment. The thermogravimetric analysis showed the presence of impurities in the specimen, or lack thereof. The FTIR analysis further confirmed that the extracted membrane from SCB and BMR are cellulose by matching the resonance frequencies of the functional groups with literature. The mean and bubble pore diameter of the cellulose membranes ranged from 2.05 to 57.67µm, with mean and bubble point pressure of 4.32 to 0.31KN/m^2. The filtration efficiency of the bleached cellulose membrane ranged from 35 to 57% with flow resistance 16.2 to 51.3 mm.H_2O. Analysis of the contact angle showed that the membrane is highly hydrophilic regardless of treatment. The cell culture experiment showed that the filtered membranes after each treatment were biocompatible, non-toxic to cells and the membranes can be used as scaffolds for tissue engineering applications. Overall, cellulose extracted from SCB and BMR have great properties which makes them potential polymers for producing eco-friendly filters that can be used for face masks and also as scaffolds for tissue engineering. The extraction and fabrication processes are safe and will also contribute to environmental sustainability.

TABLE OF CONTENTS

ILLUSTRATIONS

Figure

TABLES

ABBREVIATIONS

SARS-CoV-2 - Severe acute respiratory syndrome coronavirus 2

SCB - Sugarcane bagasse

BMR – Banana midrib

FA – Formic acid

AA – Acetic acid

PFA – Performic acid

PAA – Peracetic acid

KSCN - Potassium thiocyanate

NMMO - N-Methylmorpholine-N-oxide

TBAF - Tetra-n-butylammonium fluoride

TFA - Trifluoroacetic acid

DCE - 1,2-dichloroethane

DMAc - Dimethylacetamide

SEM – Scanning electron microscope

TGA – Thermogravimetric analysis

FTIR – Fourier transform infrared spectroscopy

PPE - Personal protective equipment

PEO - Polyethylene oxide

PP – Polypropylene

$NaClO_2$ - Sodium chlorite

NMR - Nuclear magnetic resonance

P - Pressure

γ - Surface tension of the Galwick wetting fluid

θ - Contact angle of the wetting fluid with the sample = 0

D - Pore size diameter

W_1 - Weight of the moist raw material

W_2 - Weight of the dried raw material

CHAPTER 1

INTRODUCTION

1.1 Background of the study

Face masks are personal protective equipment that are the mainstay of protection against airborne pathogens such as severe acute respiratory syndrome coronavirus 2 (SARS-CoV-2 or Covid-19) and adsorbing toxic/hazardous gases[1]. These masks can filter out at least 40% of microscopic particles of 300nm in size[2]. The various components of the mask include an air filter, nose adapter, and elastic ear loops [3]. Each component is constructed of a different material, such as polypropylene or polyester for the filter, aluminum for the nasal adapter, and cotton for the elastic loops. In March 2020[4], an unprecedented scarcity of personal protective equipment (PPE) for everyone (including clinicians and key health care workers) occurred, resulting in an increase in the frequency of SARS-COV-2 virus transmission and a high mortality rate. According to recent studies, over 129 billion face masks are used globally every month[5] since the commencement of Covid-19 pandemic, and the manufacturing of these masks necessitates a large consumption of fossil-based materials and the generation of large amounts of toxic waste, both of which can result in environmental pollution, infection and ozone layer depletion[5-8].

Furthermore, masks are difficult to recycle, making product end-of-life management a critical and impactful aspect to manage, as the majority of masks end up being discarded in municipal solid waste landfills, rivers, or incinerated[9] resulting in greenhouse gas emissions[8], infection or death of aquatic microorganisms, and the potential for re-entry into the human food chain, causing severe health problems. Several

studies are being supported to obtain biodegradable masks, which should make end-of-life disposal easier while also contributing to a sustainable environment.

1.2. Problem statement

Environmental sustainability has long been a major global concern that encouraged research in different fields of study. Environmental sustainability involves scrap recycling, organic solid waste recycling, and a reduction in reliance on fossil fuels among others. The development of biodegradable biomaterials has significant promise for addressing many sustainability issues, as they have the potential to be renewable, biodegradable, and free of toxic chemicals[10]. Furthermore, farm waste products including banana mid-rib (BMR), banana rachis, sugarcane bagasse (SCB), cassava stem constitute a major source of solid organic waste resulting in a considerable amount of by-products that pollute the environment [11]. After fruits are gathered from the farm, farmers discard any pieces that do not appear to be useful, resulting in a massive amount of waste, a deficit of income for farmers, and environmental pollution that can contribute to public health issues and ozone layer depletion. These farm products can be processed into valuable biodegradable polymers (e.g., cellulose, lignin), providing farmers with additional revenue and contributing to a more sustainable environment.

Cellulose is a naturally occurring polymer. It is biocompatible, biodegradable, and the most abundant renewable biopolymer on the planet[12], making it one of the best alternatives to synthetic polymers (e.g. polypropylene, polyester etc.). These characteristics make cellulose fibers suitable for a variety of applications, including filtration, artificial tissue/skin, protective and water-resistant garments and wound healing among others. In cotton fibers, cellulose is almost pure, while in plants, it is present in combination with other basic components such as lignin and hemicelluloses[13]. Examples

of this farm products include sugarcane bagasse (which consists of 23.5% lignin, 28.6% hemicellulose, and 43,8% cellulose)[14], banana stem (which contains 18% lignin, 32% hemicellulose, and 50% cellulose)[15], rice (25-30% lignin, 15-20% silica, and 50% cellulose) etc. Recent studies have focused on overcoming environmental issues such as developing a cellulose-based absorbent for oil spills and heavy metal pollution on water or land[16], as well as developing filters for industrial pollution[17], health care air-borne infections, and municipal waste-water treatment[18].

1.3 Aims and objectives

The goal of this study is to extract cellulose from sugarcane bagasse (SCB) and banana mid-rib (BMR), conduct characterization analysis on cellulose extracted from SCB and BMR, and use the derived cellulose to create an eco-friendly filter.

CHAPTER 2

LITERATURE REVIEW

Polypropylene, polyacrylonitrile, polycarbonate, polyurethane, polystyrene, polyester, and polyethylene are popular polymers used in the manufacture of face masks. Non-biodegradable masks are made from these materials by a spun-bonding and melt-blowing method, which has a negative impact on people's health and aquatic habitats[19, 20]. Sneha et al. 2019[20] electrospun polyvinyl alcohol (PVA), graphene, and hydroxyapatite to manufacture a mask. This mask can absorb hazardous and polluting gases from particulate matter like vehicle emissions, industrial exhausts, incinerators, mosquito coils, and so on. The non-biodegradable feature of electrospun PVA, graphene, and hydroxyapatite fibers, as well as their inability to filter particulate matter smaller than 3.5 µm, are the fibers' limitations[20, 21].

By electrospinning chitosan and polyethylene oxide (PEO) blend solutions onto a spunbonded non-woven polypropylene (PP) substrate, Keyur et al. 2009[22] fabricated a nano-fibrous filter media. Chitin, the second most prevalent polysaccharide found in the exoskeleton of crustaceans, crabs and shrimp shells, insects, and fungal mycelia, was used to make chitosan[23]. However, due to the dense structure of the PP mat, electrospinning a continuous layer of chitosan fibers on melt-blown PP webs was not practical. The successful synthesis of chitosan-based nano-fibrous filter media was achieved by electrospinning chitosan blend solutions on spunbonded PP substrates. The nano-fibrous filter media containing chitosan has the benefit of filtering material based on both its size and functionality. It is also potentially applicable in a wide variety of filtration applications ranging from water purification media to air filter media. The

limitations of electrospun fibers fabricated by Keyur et al., is that the nano-fibrous layer lacks mechanical strength to withstand pressure and the filtration efficiency is unknown[22].

Cellulose has been used by numerous researchers for various purposes due to its vast availability, and there are several methods developed to extract cellulose from farm products. According to Kanchireddy et al.[24], ficus leaf fibers can serve as an alternate raw material for the extraction of cellulose. By using the acid chloride-soda approach, cellulose was successfully extracted from the ficus leaves' fibers. Fourier Transform Infrared (FTIR) and Nuclear Magnetic Resonance (NMR) analyses of the extracted cellulose revealed the removal of hemicellulose, lignin, and other impurities due to the extraction process. According to the results of the chemical analysis, the amount of extracted cellulose due to various treatments rose from 38.1 to 84.8 percent[24] and the thermogravimetric examination showed that the extracted cellulose is more thermally stable than the raw fiber.

The extraction of cellulose from natural areca fiber was explored by Rague et al. in 2019[25]. Using formic acid and hydrogen peroxide, cellulose was extracted from areca fiber, yielding 65% cellulose, 30% hemicellulose, and 5% lignin. The lignin and hemicellulose in this process of extraction diminish the crystalline quality of the cellulose, making it impossible to electrospin the impure cellulose obtained. Andres et al. as well as other researchers discussed how lignin and hemicellulose can be extracted from cellulose, and how cellulose can be processed as thermoplastic elastomers[26], natural wood adhesives[27], high performance broad spectrum sunscreen[28], and pressure sensitive adhesive[29] among several other applications, due to the numerous phenolic groups and high molecular weight of lignin.

Being a stiff polymer with close chain packing, cellulose has been described as particularly difficult to dissolve without chemical modification or derivatization. Cellulose dissolution is a lengthy, multistep process and scientists are making great efforts to speed up the process of dissolving cellulose extracted from different sources such as wood pulp, bamboo pulp, and ramie pulp among others [30, 31] using organic or ionic solvents. N-methyl morpholine-N-oxide (NMMO) (Figure 1) is the only cellulose solvent used commercially to produce textile fibers through the Lyocell processes[32, 33] because it is environmentally friendly, fully biodegradable, non-toxic and non-ecotoxic[34-36]. This technology was established by American Enka and Eastman Kodak and later commercialized by Courtaulds[37]. NMMO has a melting temperature of 170 °C and it is solid at room temperature. Anwar et al. 2019[38], dissolved cellulose pulp using NMMO solution under the process of Lyocell slurry. The optical weight and thickness gain, scanning electron microscope (SEM), and X-ray diffraction (XRD) measurement techniques are used, respectively to describe the dimensions, interstitial spaces, and crystallinity of the structural changes of pulp in Lyocell slurry at various temperatures. Margaret et al. 2006[31] investigated the dissolution of cellulose in ethylene diamine (EDA) and potassium thiocyanate (KSCN) solution by infrared spectroscopy (FTIR) and differential scanning calorimetry (DSC) using freeze thaw cycling and vortex of mixtures methods. The result revealed that mixing was important for formation of homogenous solution and freeze thaw cycling was not. The major limitation of using EDA as a solvent is that EDA is corrosive with an ammonia-like odor and is a respiratory irritant. Other recent used solvents, including dimethyl sulfoxide (DMSO), tetra-n-butylammonium fluoride (TBAF)[39, 40] or ionic liquids[41], can dissolve cellulose without the need for

activation or pretreatment, but they have disadvantages such as being expensive (DMSO/TBAF, NMMO) or toxic (EDA, trifluoroacetic acid).

By electrospinning post-treated liquified banana stem with hydroxyapatite nanocrystals, Mehdi and Milad created a bone scaffold for tissue engineering applications [42, 43]. Meng et al. 2019[44], described a method for extracting liquid residue from the banana pseudo-stem , and the liquefied residue was subsequently bleached with acidified sodium chlorite ($NaClO_2$). The cellulose polymer was electrospin after being dissolved in a combination of trifluoroacetic acid (TFA), 1,2-dichloroethane (DCE), and dimethylacetamide (DMAc). The limitation of this method is that TFA is a caustic and corrosive solvent[45] which could injure the bone even more and reduce the quality of life.

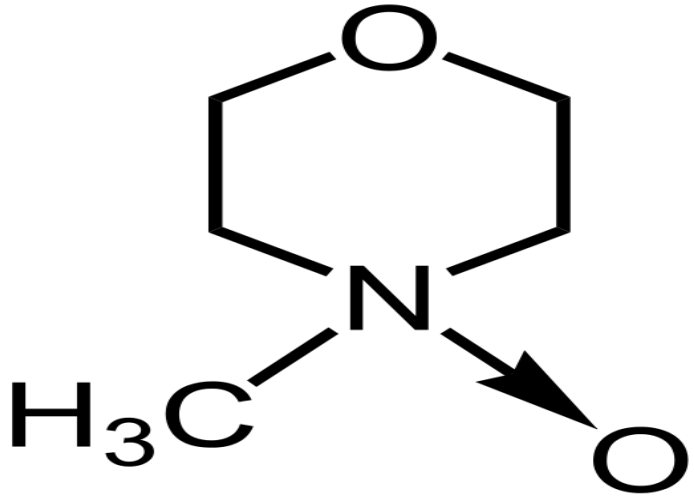

Figure 1. Chemical structure of N-methyl morpholine-N-oxide (NMMO)

CHAPTER 3

MATERIALS AND METHODS

3.1 Materials

SCB and BMR are the natural raw materials utilized. The chemicals utilized include sodium hydroxide (Sigma, Germany), ethanol (J.T.Baker, Poland), distilled water, hydrogen peroxide (Sigma, Germany), formic acid (Fisher, Belgium) acetic acid (Sigma, Germany) , performic acid (Merck, Germany), peracetic acid (Merck, Germany), Trifluoroacetic acid (Fisher, Belgium), ethylene diamine (Sigma, USA)), and potassium thiocyanate (Flinn, USA).

3.2 Experimental procedure

Sugarcane bagasse and banana midrib are complex plants, and their impurities can interfere with the concentration of cellulose and ultimately reduce the final product quality[46]. The percentage composition of SCB includes 44.6% cellulose, 33.5% hemicellulose, 18.1% lignin, 2.3% ash, 0.8% wax, and 0.7% other impurities[47]. The banana midrib contains 60.6% cellulose, 12.4% hemicellulose, 18.9% lignin, 2.9% ash and 5.2% other impurities[48, 49]. The experimental procedure explains how cellulose fibers were extracted from SCB and BMR in four treatment stages.

3.2.1 Treatment of SCB and BMR by boiling i.e., Basic treatment

The first step was the collection of the natural raw materials (i.e., SCB and BMR) from local farmers. Then 400g of SCB and BMR were weighed separately, dried using an oven at a temperature of 75°C for 6-8 hours. The final weight was measured and the

percentage moisture content of SCB and BMR were calculated using the formulae below[50];

Percentage Moisture content of SCB/BMR=

$$\frac{W_1 - W_2}{W_1} \times 100 \qquad \text{(Equation 1)}$$

$W_1 = weight\ of\ the\ moist\ raw\ material$ = 400g

$W_2 = weight\ of\ the\ dried\ raw\ material = 212g$

Percentage moisture content of SCB/BMR=

$$\frac{400 - 212}{400} \times 100 = 47\%$$

After obtaining dried SCB and BMR, it was grinded using Pulverisette25 of 2mm trapezoidal perforator to obtain a fine homogenous material. A sodium hydroxide (NaOH) pellet at 8g was added to 75% water, 25% ethanol (EtOH) and 3g of each grinded sample (SCB and BMR). The resulting solution was placed on a hot stirrer for 10 hours while it boils and stirs, maintaining a solution temperature of 95°C (figure 2). The cooled solutions were sonicated for 10 minutes at an amplitude of 90%.

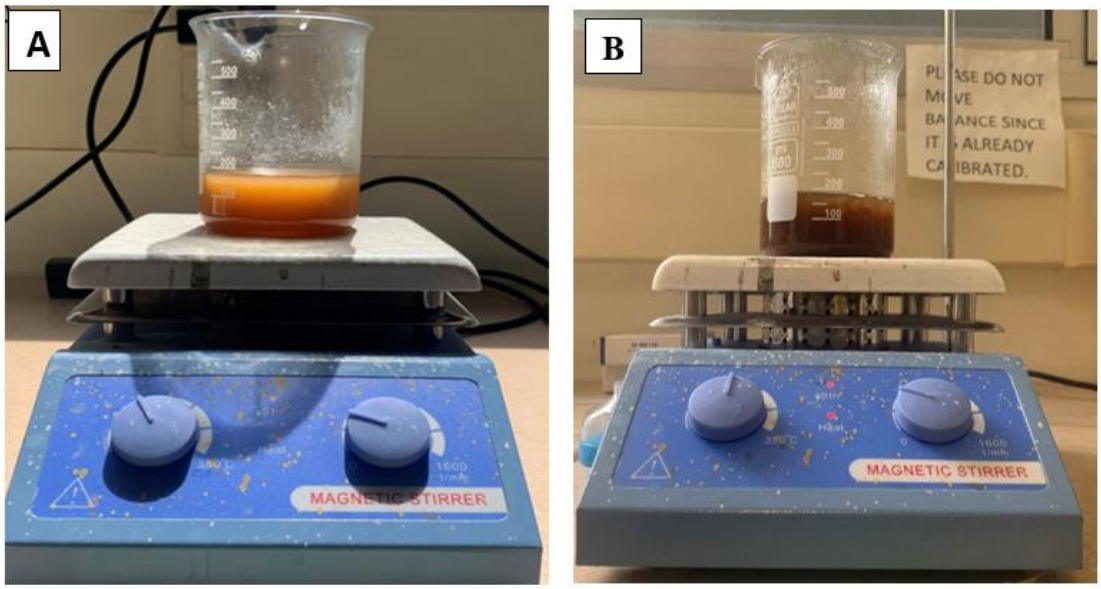

Figure 2. Boiling for 10 hours to disrupt the cell wall of hemicellulose, cellulose and lignin: (a) 3g SCB+8g NaOH+75% water+ 25% EtOH (b) 3g BMR+8g NaOH+75% water+ 25% EtOH

3.2.2 Treating SCB and BMR with 70% Formic acid (FA) and 30% Acetic acid (AA)

A mixture of 50% organic acid (containing 70% FA and 30% AA) was added to the sonicated SCB and BMR pulp solution respectively and it was boiled for 2hours. After 2 hours, the flask and its contents were allowed to cool to ambient temperature. The solutions were filtered using a Buchner funnel (figure 3), and the filtered fibers were washed with formic acid (FA) followed by hot distilled water (figure 4).

Figure 3. Filtration setup

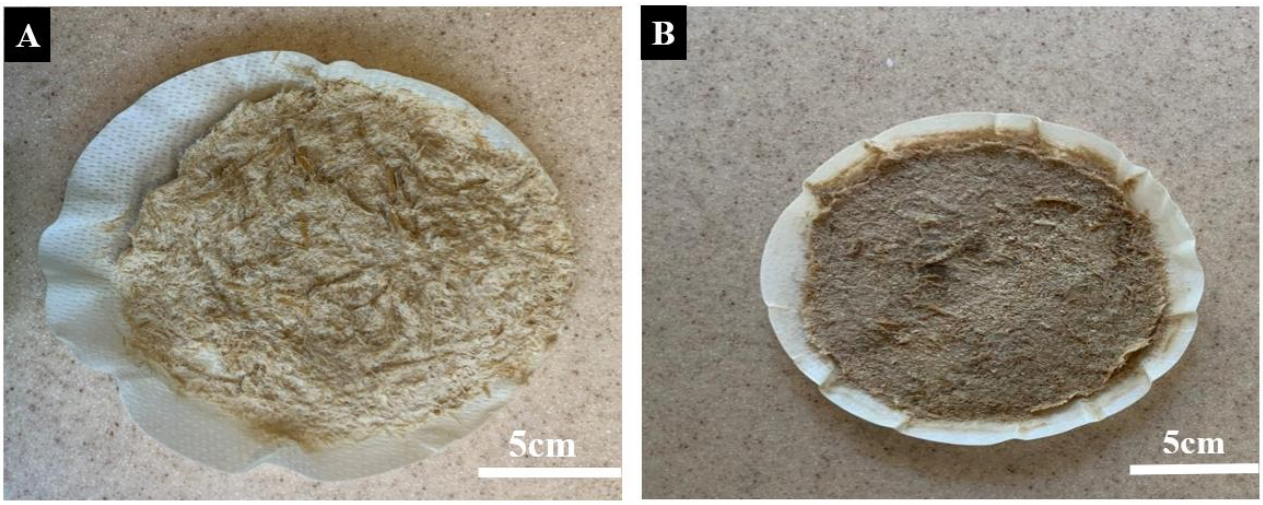

Figure 4. Filtered (A) SCB and (B) BMR after 2 hours of boiling with 70% Formic acid and 30% Acetic acid

3.2.3 Treating SCB and BMR with Performic acid (PFA) and Peracetic acid (PAA) i.e., Advance treatment

The fibers were further treated using mixture of PFA and PAA (i.e., 56% FA, 24% AA and 20% H_2O_2) maintaining a boiling temperature of 60°C for 2 hours to obtain delignified fibers. The delignified fibers were filtered to separate the liquor impurities

(containing lignin, hemicellulose, PFA, and PAA) from cellulose and washed with hot distilled water.

3.2.4 Bleaching

The delignified fibers were mixed with 70% distilled water and 30% hydrogen peroxide (H_2O_2) solutions for bleaching by boiling the mixtures at 80°C for 2 hours (figure 5). Finally, the pulp was washed with distilled water to remove residual lignin and other impurities. This process was repeated to remove lignin completely. We obtained 8 different samples which are:

sample 1: SCB + NaOH + EtOH

sample 2: SCB + NaOH + EtOH / FA+AA

sample 3: SCB + NaOH + EtOH / FA+AA / FA+AA+H_2O_2

sample 4: SCB + NaOH + EtOH / FA+AA / FA+AA+H_2O_2 / H_2O_2

sample 5: BMR + NaOH + EtOH

sample 6: BMR + NaOH + EtOH / FA+AA

sample 7: BMR + NaOH + EtOH / FA+AA / FA+AA+H_2O_2

sample 8: BMR + NaOH + EtOH / FA+AA / FA+AA+H_2O_2 / H_2O_2

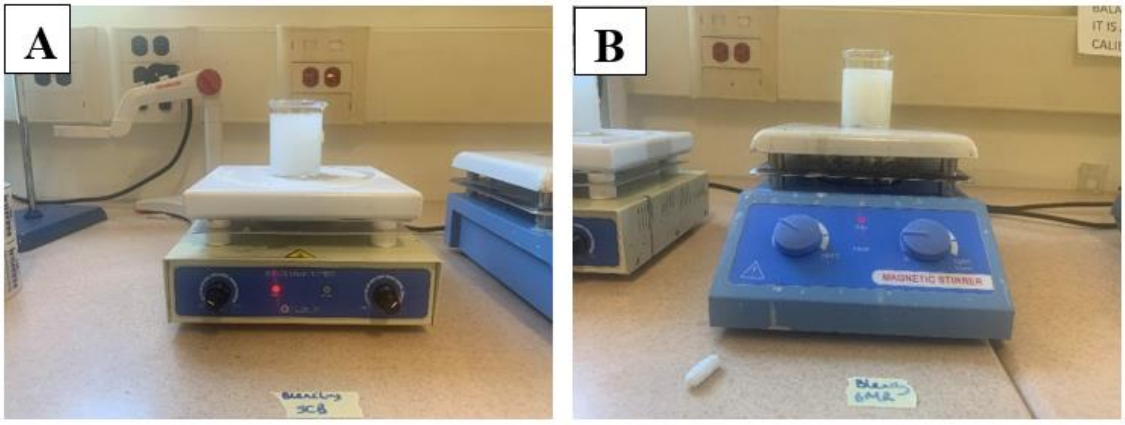

Figure 5. Bleaching of extracted fiber from (A) SCB and (B) BMR

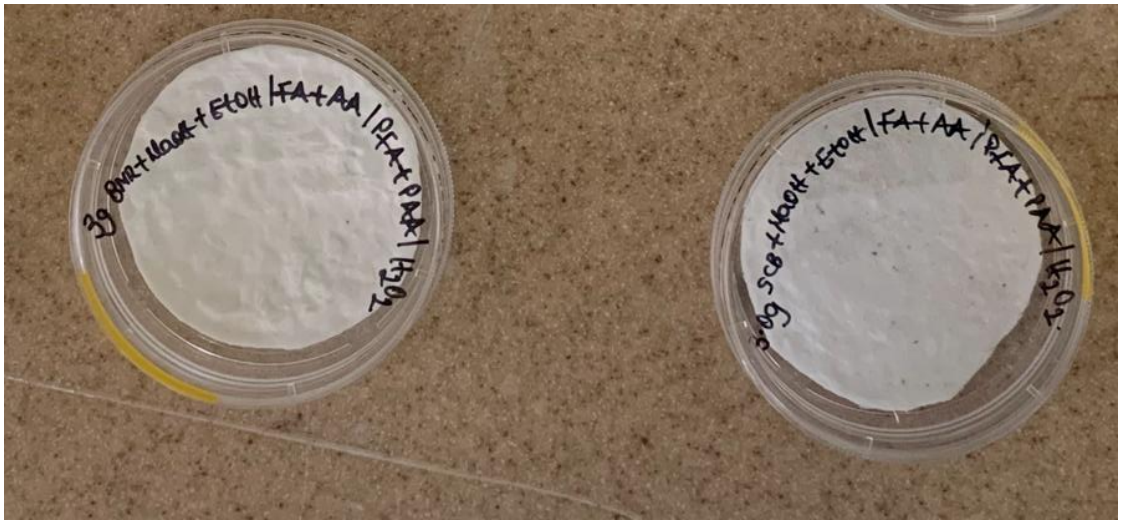
Figure 6. Bleached cellulose membrane extracted from BMR and SCB

3.3 Characterization

Various characterization analysis were performed on the samples to know the most potential material for fabrication of the filter. The characterization analysis conducted include scanning electron microscopy (SEM) analysis, thermogravimetric analysis (TGA), Fourier transform infra-red (FTIR) spectroscopy analysis, porosity test, mechanical test, contact angle measurement, filtration efficiency test, and flow resistance analysis.

3.3.1 SEM analysis

The samples were mounted on conductive adhesive tape, then coated with 10µm gold nanoparticle using the sputtering machine. The SEM was used to examine the microstructure of the samples using a voltage of 5.0KV.

3.3.2 TGA analysis

Thermo-gravimetric analysis (TGA) was used to determine the thermal stability and decomposition temperature of various impurities present in SCB and BMR after

subjection to different treatments. From each sample, 10mg were heated from ambient temperature to 600°C at the rate of 10°C/minute under nitrogen atmosphere using platinum pan as sample carrier.

3.3.3 FTIR analysis

The functional group of the post-treated fibers extracted from SCB and BMR were analyzed using FTIR by heating the samples from temperature of 30 to 600°C at a rate of 10°C/minute under nitrogen atmosphere using alumina crucible as sample carrier.

3.3.4 Porosity analysis

The average thickness of the cellulose membrane (i.e., sample) was measured using thickness gage (figure 7). The mean flow pressure, flow diameter, bubble point pressure, bubble point pore diameter and flow rate of cellulose extracted from SCB and BMR were characterized using capillary flow porometer CFP-1100AH and Galwick™ solution was used as wetting fluid.

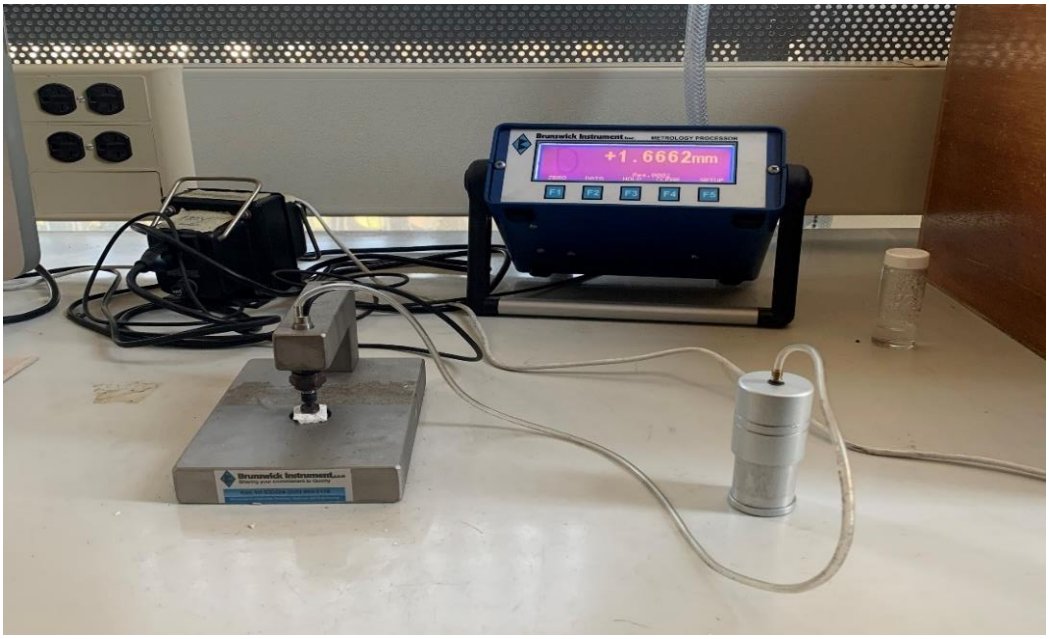

Figure 7. Membrane thickness measurement gauge

3.3.5 Mechanical testing

Mechanical testing was carried out on the extracted cellulose membranes using a universal testing machine (UTM). Tensile tests were conducted on specimens cut from the treated membranes at a strain rate of 5mm/sec. The specimens had widths of 15mm, and length 43mm. The thickness was measured for each sample individually.

3.3.6 Contact angle measurement

The contact angle measurement was carried out to evaluate wettability characteristics of the membrane after each treatment. This wettability property was done using an optical tensiometer. The machine uses SCA20 software to control the experiment and analyze drop shape to calculate contact angle. 6.0µL of deionized water was dispensed on the sample using an automatic dispenser at a dosing rate of 1.0µL/s and at ambient temperature.

3.3.7 Filtration Efficiency and Flow resistance measurement

The filtration efficiency and flow resistance of the treated samples were assessed using a condensation particle counter TSI model 3772 in line with a classifier TSI 3082 (figure 8). The setup was made with a glass rectangular box having provisions to hold the specimen, connect condensation particle counter and classifier TSI across the specimen. For the filtration and flow resistance measurement, a glass jig acting as a mannequin was connected to a cylindrical aerosol sampling station at one end while the other end was used for air suction without and through the treated sample. After validating the set-up and the methodology, the samples were employed as test specimens.

Figure 8. Scanning mobility particle sizer spectrometers setup

3.3.8 Dissolution of extracted cellulose

The extracted cellulose was dissolved in 2.5, 4.0, 5.5 and 7.0 weight percent of ethylenediamine and potassium thiocyanate using freeze thaw and vortex methods for electrospinning.

3.4 Membrane biocompatibilty test

To evaluate the membrane's biocompatibility and toxicity as a scaffold for tissue engineering application, MD-MB-231 cells were cultured on the extracted membranes inside a 24-well cell culture plate. The live and dead assay of the cells were studies using calcein-AM and Ethidium homodimer dye respectively. The cells' proliferation and attachment after days 1, 2 and 3 were evaluated using Calcein-AM/Ethidium homodimer staining, and visualized under an inverted fluorescence microscope. The number of viable cells adhered to the scaffold was then quantified from the images taken.

CHAPTER 4

RESULT AND DISCUSSION

4.1 Microstructure morphology of SCB and BMR Using Scanning Electron Microscope

SEM images of the materials' microstructure are depicted in figures 9 to 12 According to the SEM images, the treatment helps to improve the samples' microstructure and produce a better network of interconnected cellulose fibers.

Treating with NaOH and EtOH causes disruption of the raw materials (i.e., sugarcane bagasse and banana midrib), making it to have junks of irregular microstructure with little or no fibers. Treatment with FA and AA further improves the microstructure of the fibers. Further treatment with PFA and PAA caused a significant improvement in the microstructure of the fibers, causing the extracted cellulose to form a significant network of interconnected fibers with little junks of impurities. The final step, which is bleaching further enhances the network and purity of interconnected fibers.

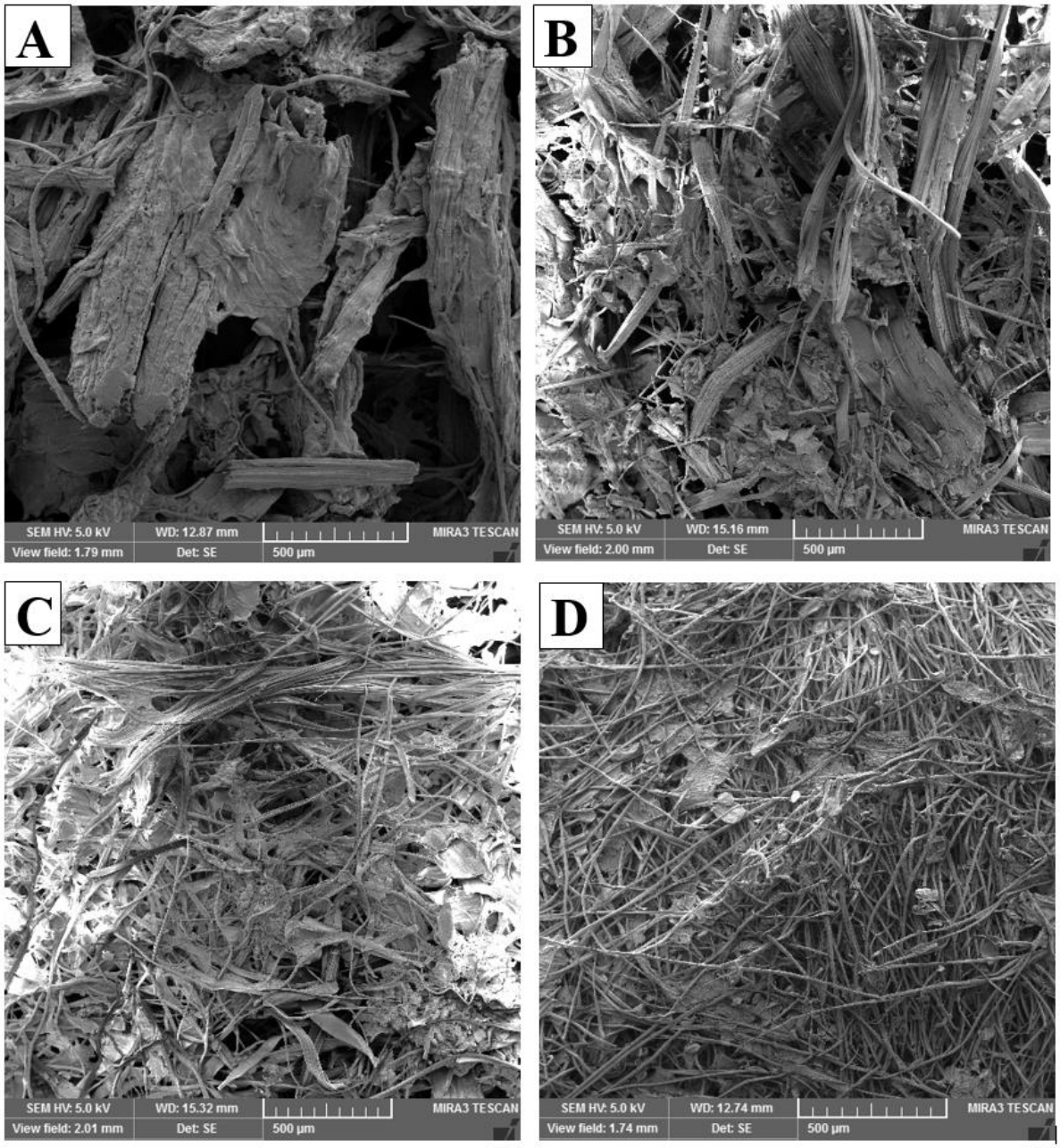

Figure 9. SEM images of SCB treated with (A) NaOH+EtOH, (B) NaOH+EtOH/FA+AA, (C) NaOH+EtOH/FA+AA/PFA+PAA (D) NaOH+EtOH/FA+AA/PFA+PAA /H2O2

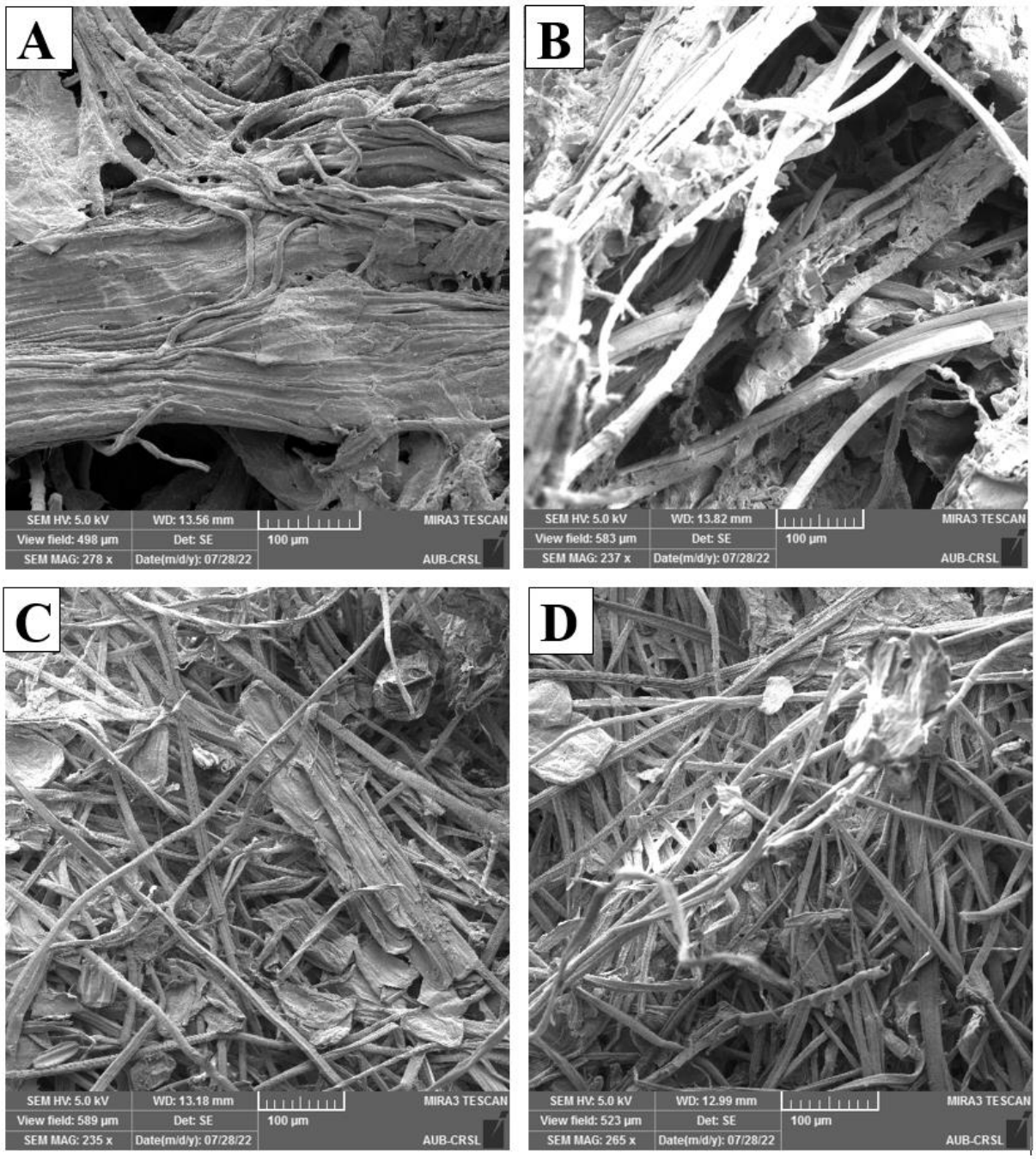

Figure 10. SEM images of SCB treated with (A) NaOH+EtOH, (B) NaOH+EtOH/FA+AA, (C) NaOH+EtOH/FA+AA/PFA+PAA (D) NaOH+EtOH/FA+AA/PFA+PAA /H2O2

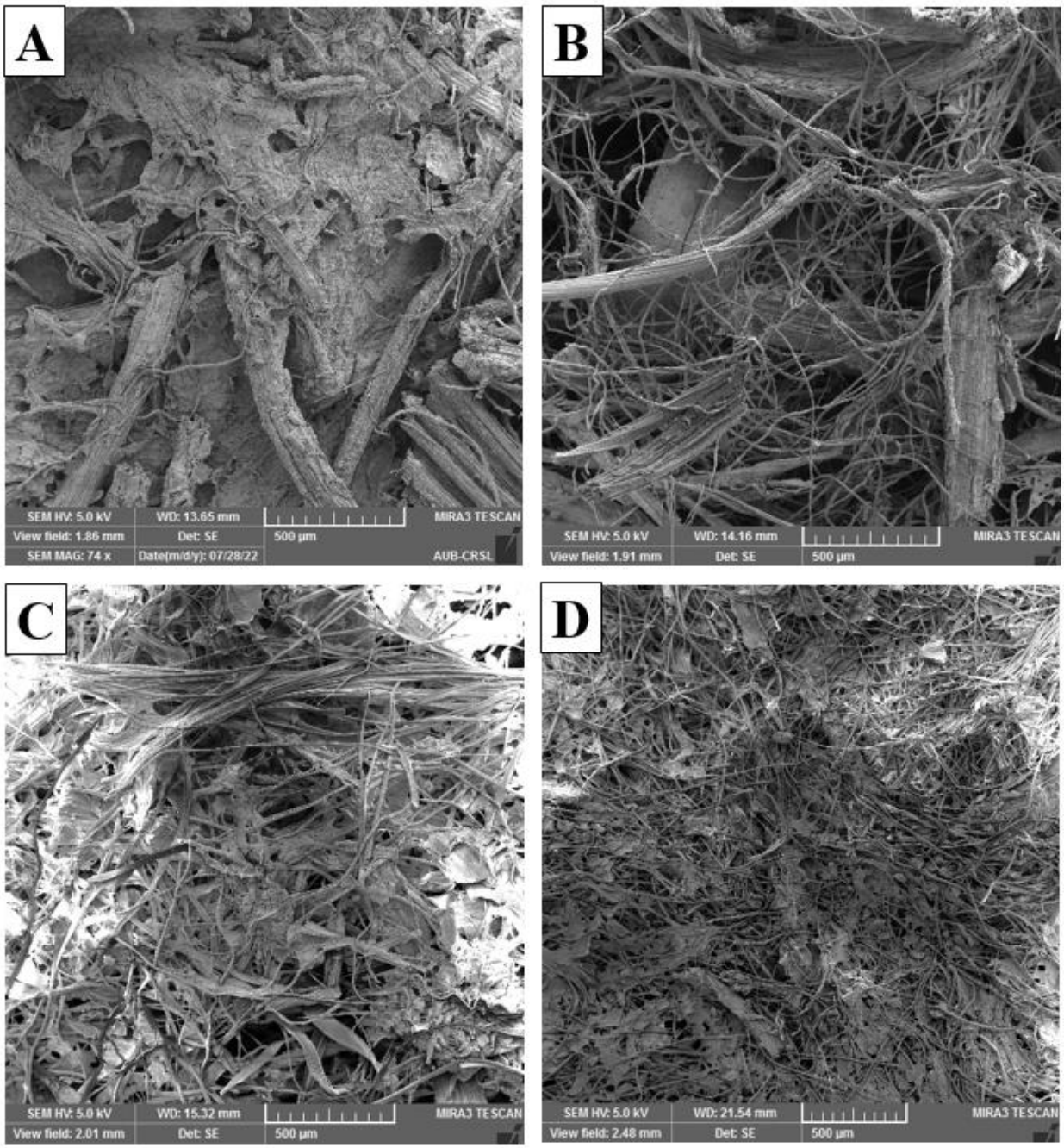

Figure 11. SEM images of BMR treated with (A) NaOH+EtOH, (B) NaOH+EtOH/FA+AA, (C) NaOH+EtOH/FA+AA/PFA+PAA (D) NaOH+EtOH/FA+AA/PFA+PAA /H2O2

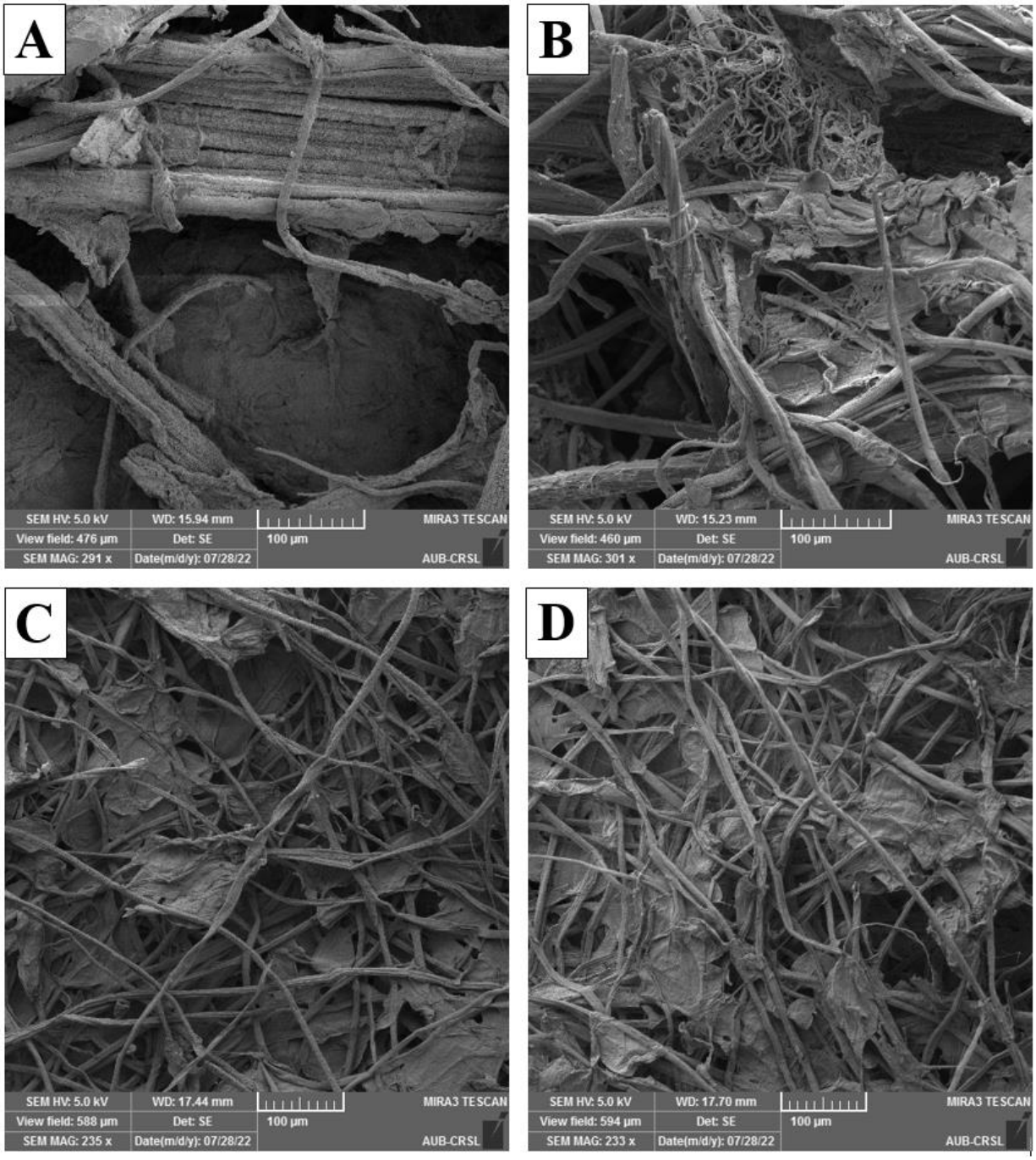

Figure 12. SEM images of BMR treated with (A) NaOH+EtOH, (B) NaOH+EtOH/FA+AA, (C) NaOH+EtOH/FA+AA/PFA+PAA (D) NaOH+EtOH/FA+AA/PFA+PAA /H2O2

4.2 Thermogravimetric analysis

TGA displays the percentage mass loss of various composites contained in each sample as a function of temperature. According to published research, lignin begins to

decompose at a temperature of about 150°C, followed by hemicellulose at 220°C, and cellulose at 315°C [51]. Figure 13 illustrates how lignin, hemicellulose, cellulose, and other impurities in SCB samples that underwent various treatments decomposed. These treatments and analysis include:

(i) The grey line graph depicts SCB treated by boiling in a mixture of NaOH, EtOH and water (i.e., **SCB+NaOH+EtOH**). Graph displays a variety of steeps; the first steep indicates that the lignin in this treated material began to decompose at a temperature of 120 °C, the second steep at a temperature of 220 °C depicts the decomposition of hemicellulose, and the final curve beginning at 300 °C indicates decomposing cellulose and other impurities that did not decompose.

(ii) The blue line graph depicts SCB that has been further processed by boiling in formic and acetic acid mixture (SCB+NaOH+EtOH/**FA+AA**). Some of the impurities started decomposing at about 100°C, hemicellulose decomposition at about 210°C, and diminish quantity of impurities compared to the first treatment.

(iii) To remove the lignin, hemicellulose, and other impurities, it was further treated by boiling in a mixture of performic and peracetic acid (i.e., SCB+NaOH+EtOH/FA+AA/**PFA+PAA**) as indicated by the red line graph. The graph shows that the impurities started decomposing at about 50°C, the cellulose started decomposing at a temperature of 315°C, and there was less quantity of impurities which failed to decompose. The graph confirmed significant elimination of lignin and hemicellulose, the presence of cellulose, and a decrease in the number of impurities that do not decompose.

(iv) As shown by the green line graph, the post-treated SCB by boiling in hydrogen peroxide (SCB+NaOH+EtOH/FA+AA/PFA+PAA/H_2O_2) began to decompose at around 315°C, which indicates that the sample is cellulose without lignin, hemicellulose, and impurities. It also demonstrates that bleaching is crucial for the complete decomposition of extracted material, removal of lignin, hemicellulose, and other impurities.

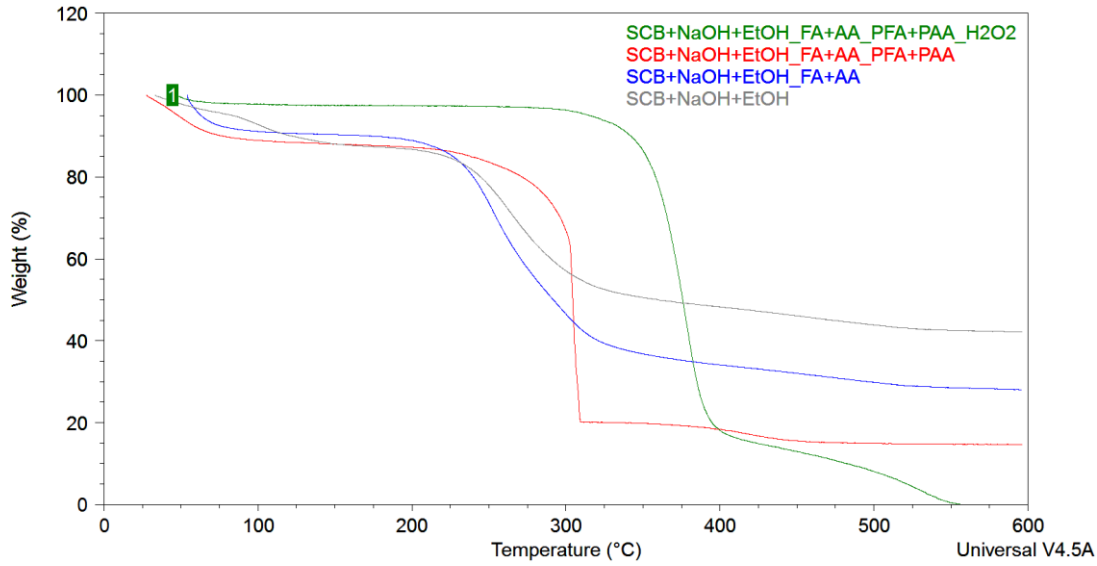

Figure 13. TGA of SCB after various treatments

Figure 14 depicts the decomposition of lignin, hemicellulose, and cellulose found in BMR samples that underwent various treatments. These treatments and analysis include:

(i) The blue line graph shows BMR after it has been processed by boiling in a solution of water, ethanol, and sodium hydroxide (NaOH) (i.e., **BMR+NaOH+EtOH**). The graph features several steps that demonstrate the decomposition of various impurities starting from about 50°C, including lignin at 120 °C, hemicellulose at 210 °C, and other impurities that didn't decompose.

(ii) The purple line graph demonstrates BMR's additional treatment, which involves boiling it in a solution of formic and acetic acid (i.e., BMR+NaOH+EtOH/**FA+AA**). The graph demonstrates significant impurities decomposition from 25°C, lignin began to decompose at 110°C, hemicellulose at around 220°C and other impurities that fails to decompose but there was reduction in the quantity of impurities compared to the basic treatment.

(iii) To remove the lignin, hemicellulose, and other impurities, it was further treated by boiling in a mixture of performic and peracetic acid (i.e., BMR+NaOH+EtOH/FA+AA/**PFA+PAA**) as indicated by the red line graph. The graph shows that the hemicellulose started decomposing at a temperature of 220 °C and some other impurities which fails to decompose.

(iv) The green line graph shows the post treated BMR by boiling in hydrogen peroxide (i.e., BMR+NaOH+EtOH/FA+AA/PFA+PAA/$\mathbf{H_2 0_2}$). The post treated extract started decomposing at about 315°C indicating that the sample is cellulose with no lignin and hemicellulose. It also shows that bleaching is

crucial for significantly removing impurities thus allowing us to reach a membrane almost completely composed of cellulose.

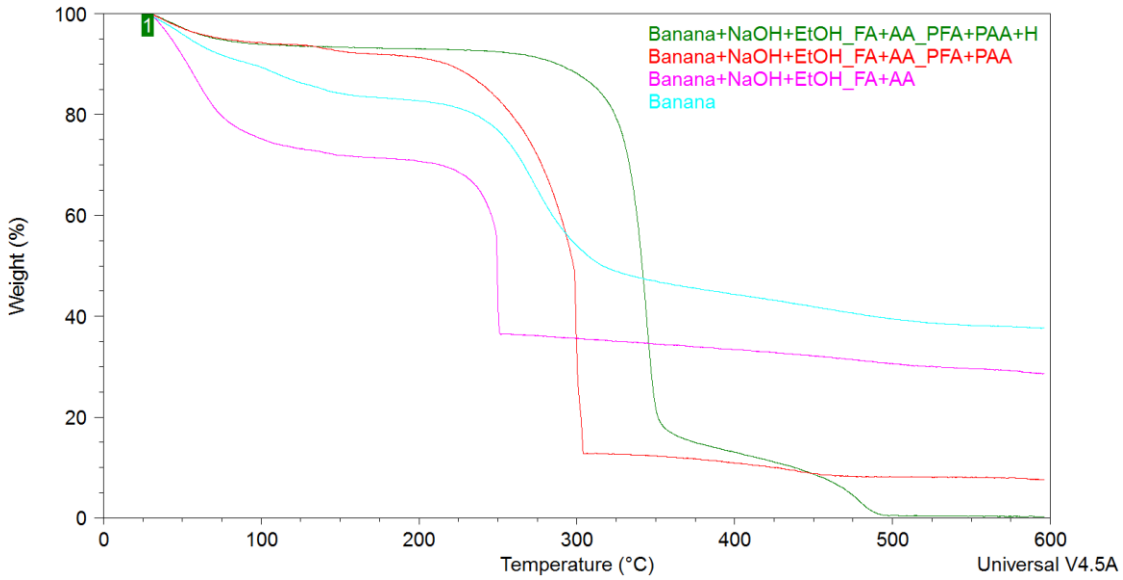

Figure 14. TGA analysis of BMR subjected to various treatments.

4.3 Functional group analysis using FTIR

Fourier transform infrared spectroscopy (FTIR) was used to analyze the functional group and interaction of bond vibration of the extracted cellulose from SCB and BMR. Figure 15 displays the FTIR spectrum of SCB cellulose. From this spectrum, the transmittance peaks of the intermolecular hydrogen bonds (O–H stretching) occurred at 3510 cm^{-1} and methylene (CH_2) stretching at 2750 cm^{-1}. The C = O stretching vibration of the carbonyl group acquired at 1720 cm^{-1}, the asymmetric stretching vibration of C–C at 1620 cm^{-1}, the H-C-H bending vibration at 1200 cm^{-1}, C-O-C pyranose ring stretching vibration at 1100 cm^{-1}, and the C–H bending vibration at 650 cm^{-1} [52-54]. Figure 16 displays the FTIR spectrum of BMR cellulose, the methylene (CH_2) stretching occur at 2600 cm^{-1}, C-O-C. The carbonyl (C=O) stretch bond occurred at 1750 cm^{-1}, the alkenes

(C=C) bonding occurred at 1400 cm^{-1}, the H-C-H bending vibration at 1150 cm^{-1}, C-O-C pyranose ring stretching vibration at 1100 cm^{-1}, and the C–H bending vibration at 500 cm^{-1}. The result of the SCB and BMR FTIR spectrum aligns closely to the FTIR spectrum of cellulose, which proves that extracted materials from SCB and BMR are cellulose[54].

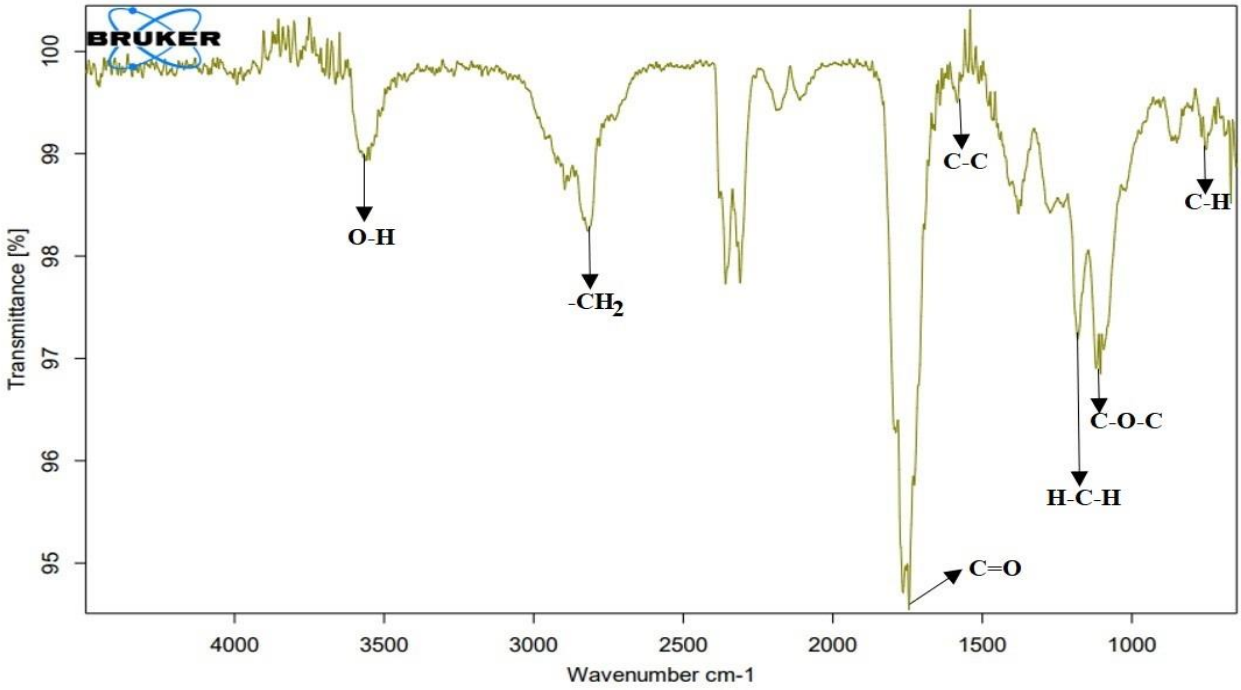

Figure 15. FTIR spectrum of membrane extracted from SCB after bleaching

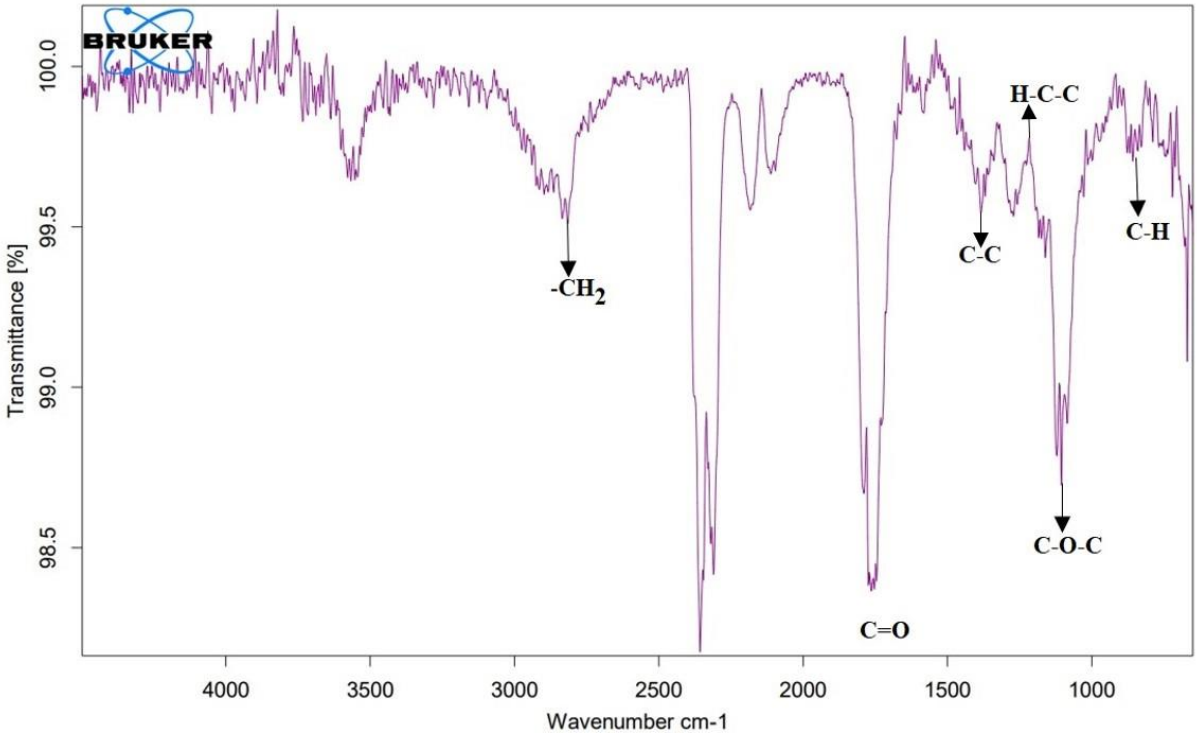

Figure 16. FTIR spectrum of membrane extracted from BMR after bleaching

4.4 Porosity analysis

The sample was placed on the membrane O-ring of the capillary flow machine after measuring it average thickness and a few drops of non-toxic wetting liquid called Galwick wetting solution was used to spontaneously fill the pores in the sample. A non-reacting gas is allowed to displace liquid from pores. More and more smaller pores are progressively emptied as the pressure increases. Finally, the pressure and flow rate of gas through the emptied pores provides the through pore distribution (figure 17).

The mean pore diameter is the average diameter of the particles that can pass through the cellulose membrane and the bubble pore diameter is the maximum diameter that can pass through the cellulose membrane, this bubble point can cause the membrane to tear. The mean and bubble point flow pore diameters and pressure of post treated cellulose fiber extracted from 3.0, 4.5, and 6.0g of SCB and BMR are shown in table 1 below.

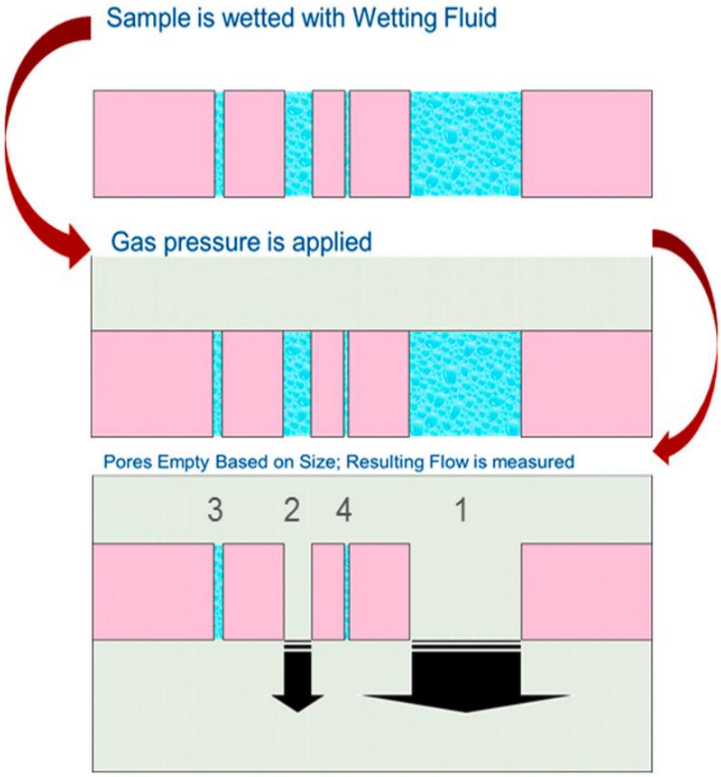

Figure 17. Operating principle of capillary flow porometer [55].

Table 1: Pore size diameter and pressure of bleached cellulose membrane from SCB

Samples	**Pore size diameter (µm)**	**Pore pressure (KN/m^2)**
3g SCB	Mean: 3.3064 BP: 22.9833	Mean: 13.761 BP: 1.978
4.5g SCB	Mean: 5.8243 BP: 39.5498	Mean: 7.811 BP: 1.151
6g SCB	Mean: 10.5318 BP: 21.5525	Mean: 4.323 BP: 0.593
Surgical mask	Mean: 4.34 BP: 10.82	Mean: 10.48 BP: 4.21

Table 2: Pore size and pressure distribution of bleached cellulose membrane from BMR

Samples	**Pore size diameter (µm)**	**Pore pressure (KN/m^2)**
3g BMR	Mean: 4.433 BP: 40.3506	Mean: 10.259 BP: 1.131
4.5g BMR	Mean: 3.9366 BP: 57.6793	Mean: 11.555 BP: 0.786
6g BMR	Mean: 2.0534 BP: 24.4516	Mean: 14.152 BP: 0.31
Surgical mask	Mean: 4.34 BP: 10.82	Mean: 10.48 BP: 4.21

The findings reveal that increasing the mass of extracted material has varying impacts on pore size diameter and pressure. The desired pore size can be achieved through electrospinning by varying the electrospinning parameter (i.e., needle diameter, flow rate, electric field, distance between the needle and collector) and solution viscosity.

The mean and bubble point pressure can also be calculated using the formula:

$$P = \frac{4 * \gamma * cos\theta}{D}$$ …… Equation 2

Where:

P = Pressure

γ = Surface tension of the Galwick wetting fluid

Θ = Contact angle of the wetting fluid with the sample = 0

D = Pore size diameter.

Figure 18-24 shows the pore distribution graph of various cellulose membrane extracted from different mass of SCB and BMR The graphs show the approximate

percentage of pores with a certain pore diameter. The results show that the initial mass used in fabricating the membrane affects the pore size and the size distribution.

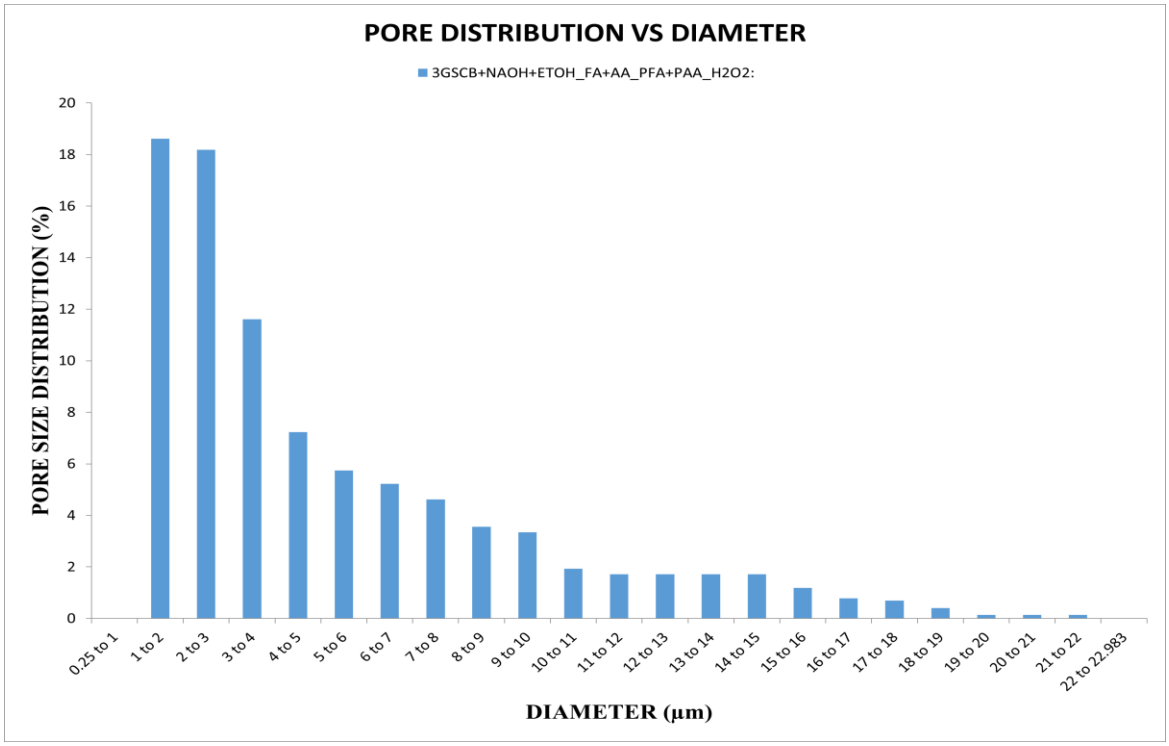

Figure 18. Pore size distribution vs diameter of cellulose membrane extracted from 3g SCB

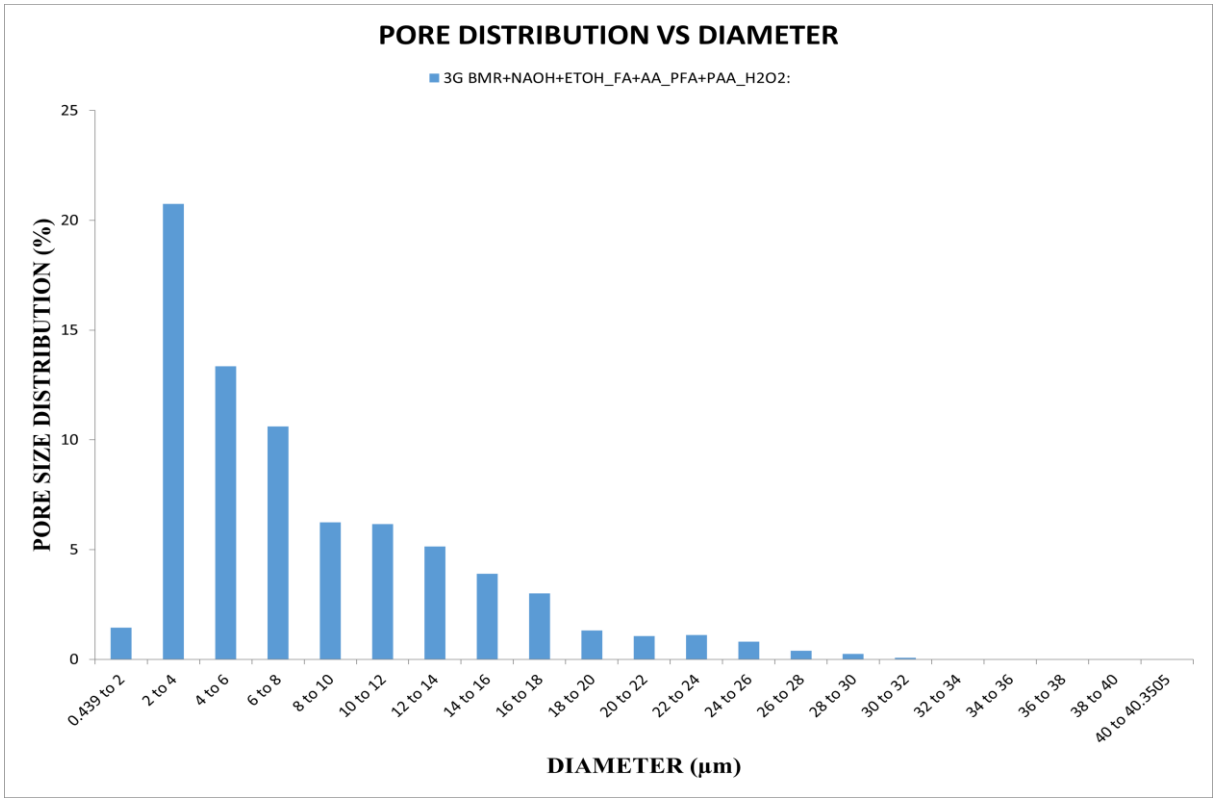

Figure 19. Pore size distribution vs diameter of cellulose membrane extracted from 3g BMR

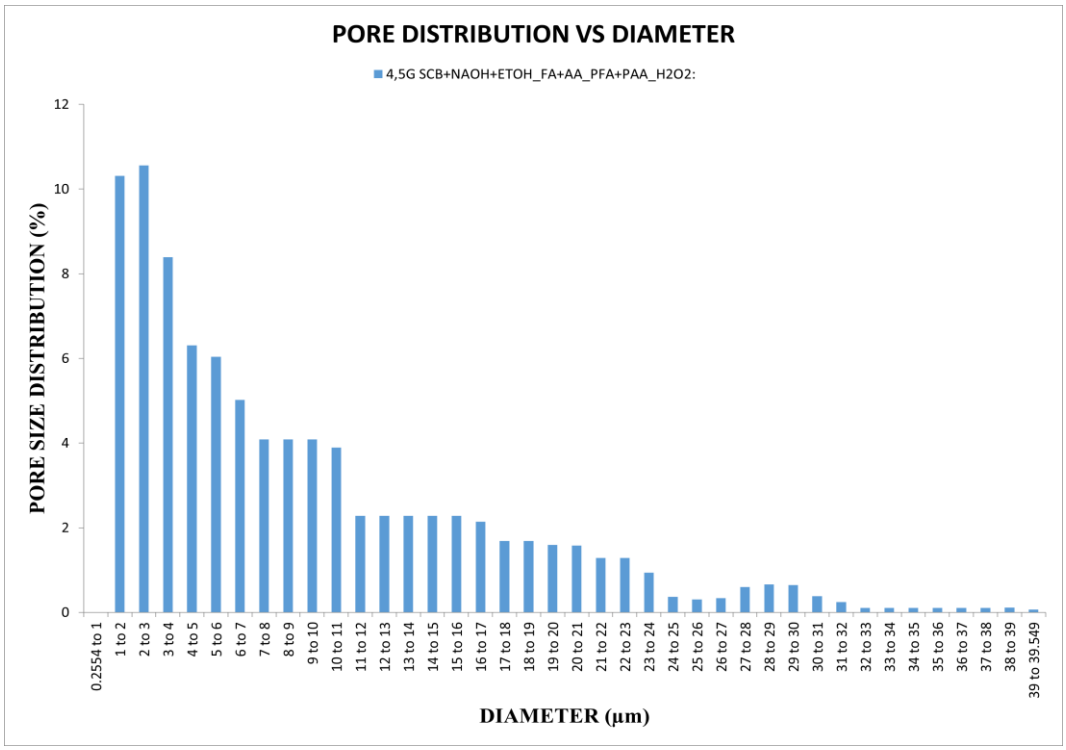

Figure 20. Pore size distribution vs diameter of cellulose membrane extracted from 4.5g SCB

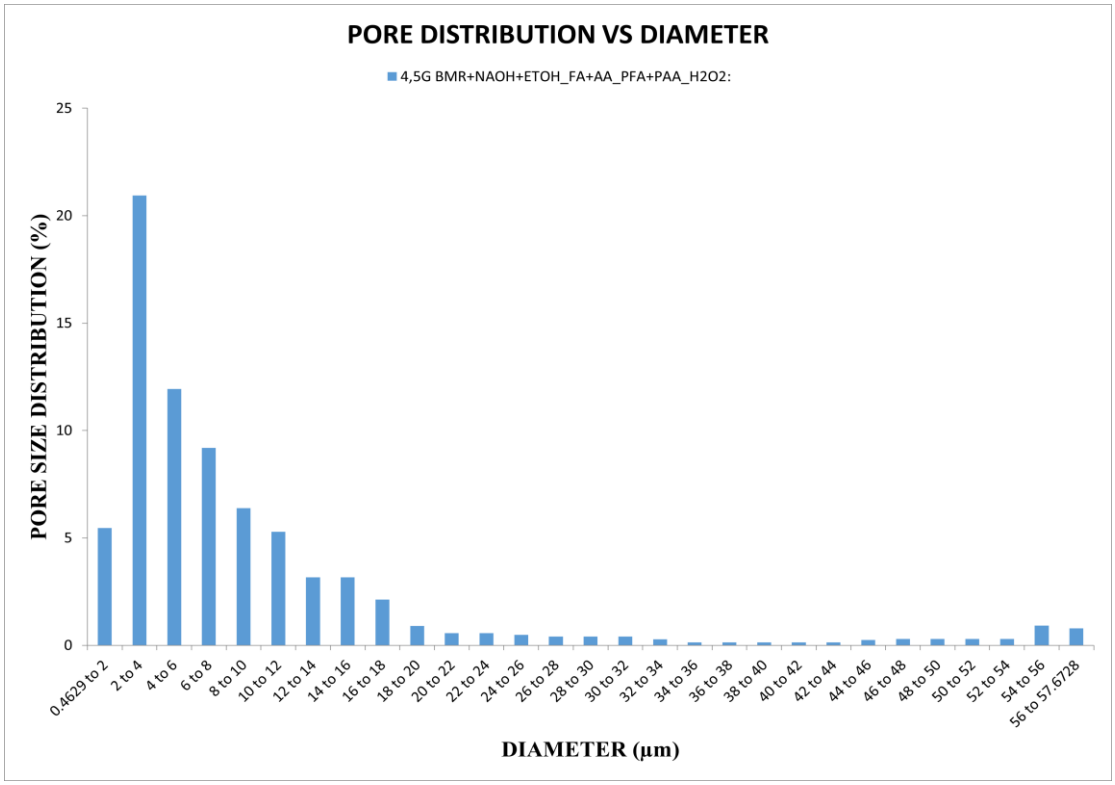

Figure 21. Pore size distribution vs diameter of cellulose membrane extracted from 4.5g BMR

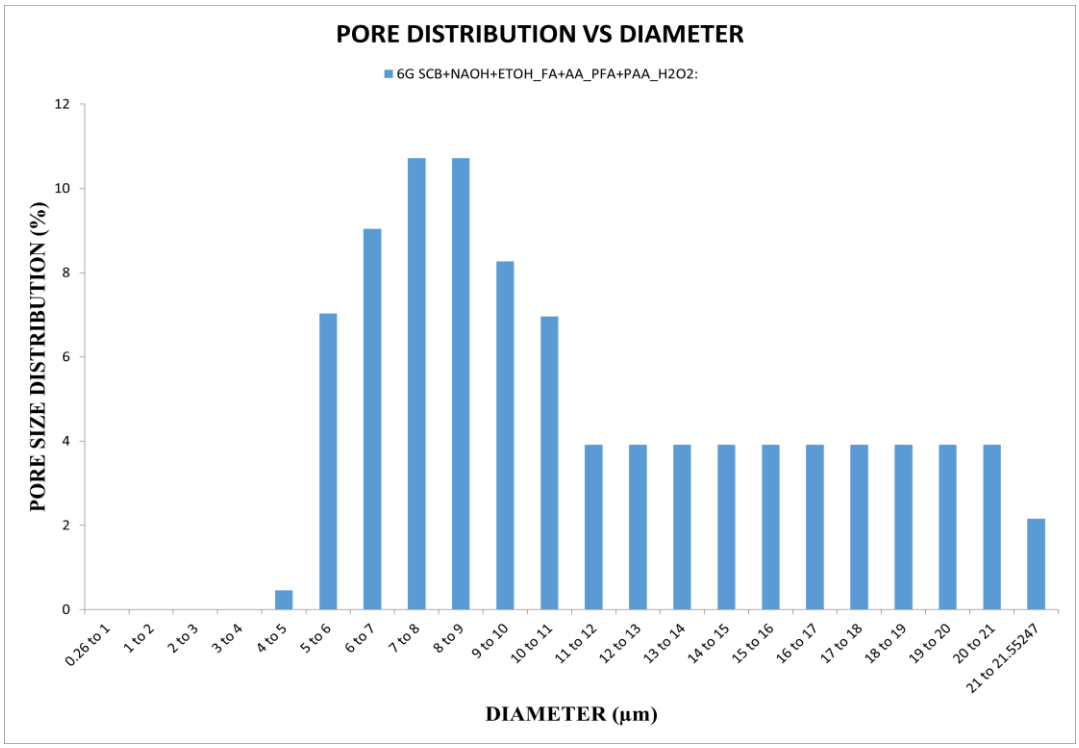

Figure 22. Pore size distribution vs diameter of cellulose membrane extracted from 6g SCB

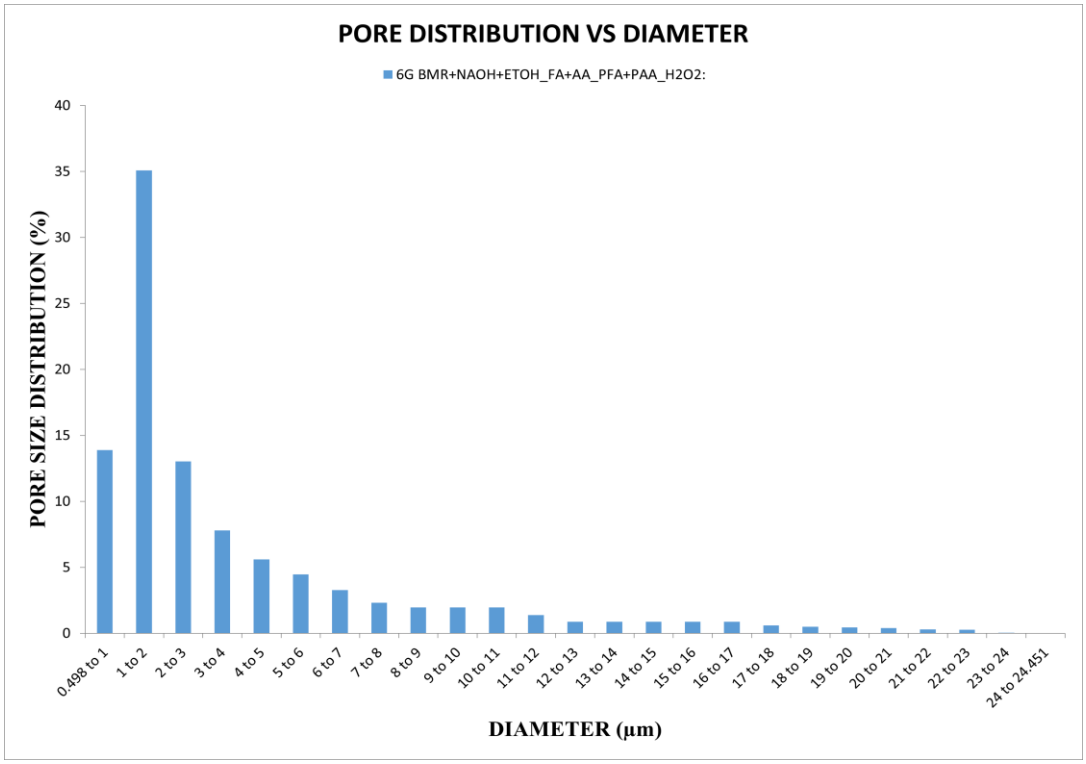

Figure 23 Pore size distribution vs diameter of cellulose membrane extracted from 6g BM

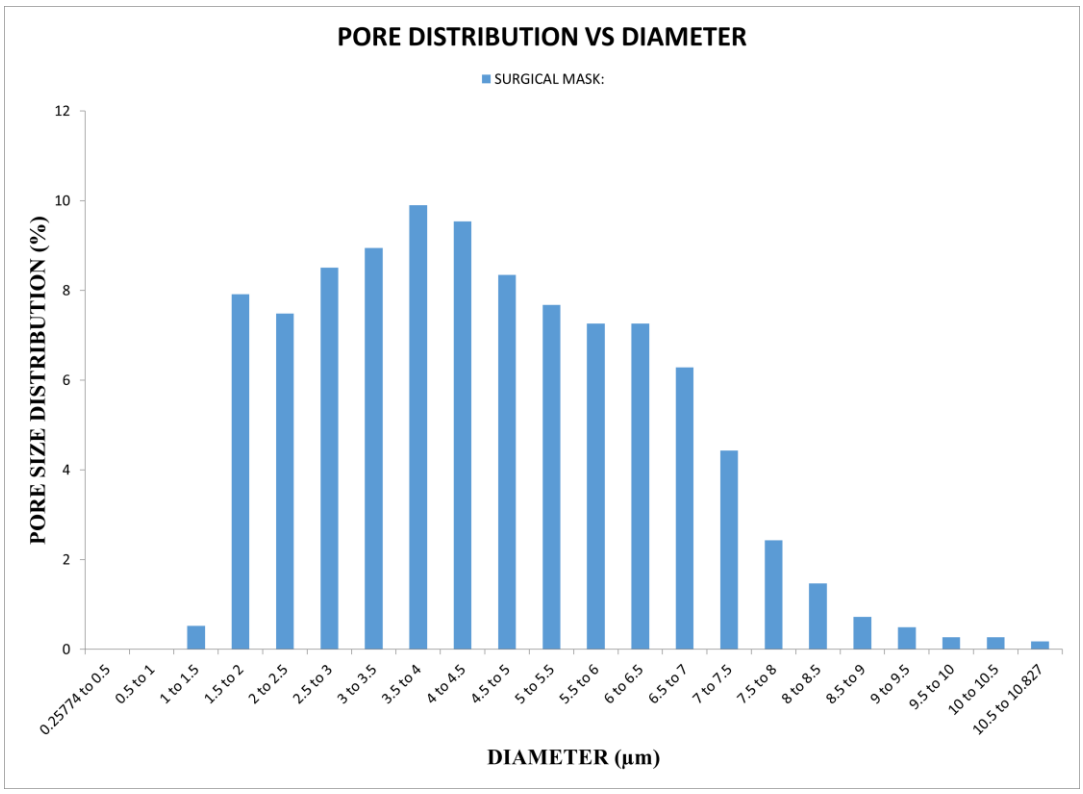

Figure 24. Pore size distribution vs diameter of surgical mask

4.5 Mechanical testing

The stress-strain curves demonstrate the relationship between the tensile stress (MPa) and tensile strain of various treatments that SCB and BMR underwent as well as how these treatments affected the membrane's strength. Mechanical testing results reveal that treating SCB and BMR with PFA and PAA significantly reduces the tensile stress of the membrane, making it exceedingly brittle. However, bleaching aids in enhancing the mechanical strength of the extracted cellulose membrane.

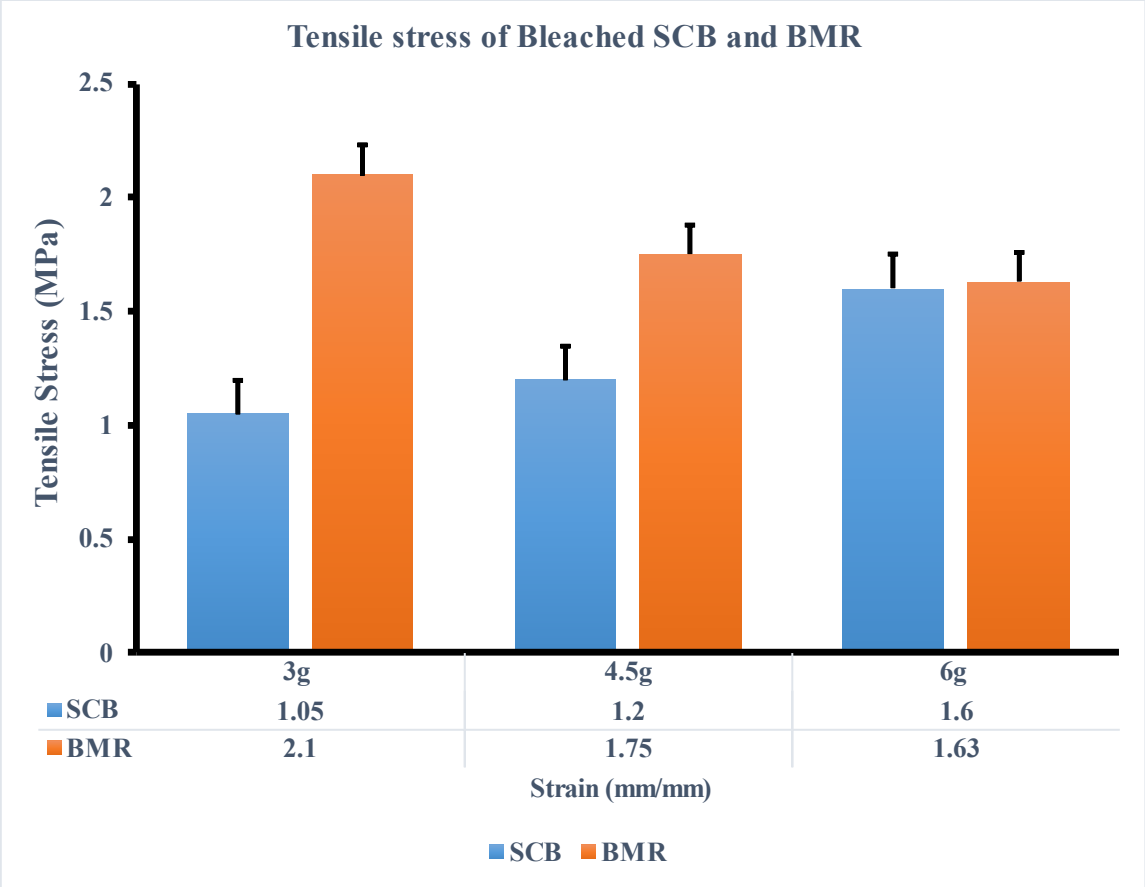

Figure 25. Maximum tensile stress of various mass of bleached SCB and BMR

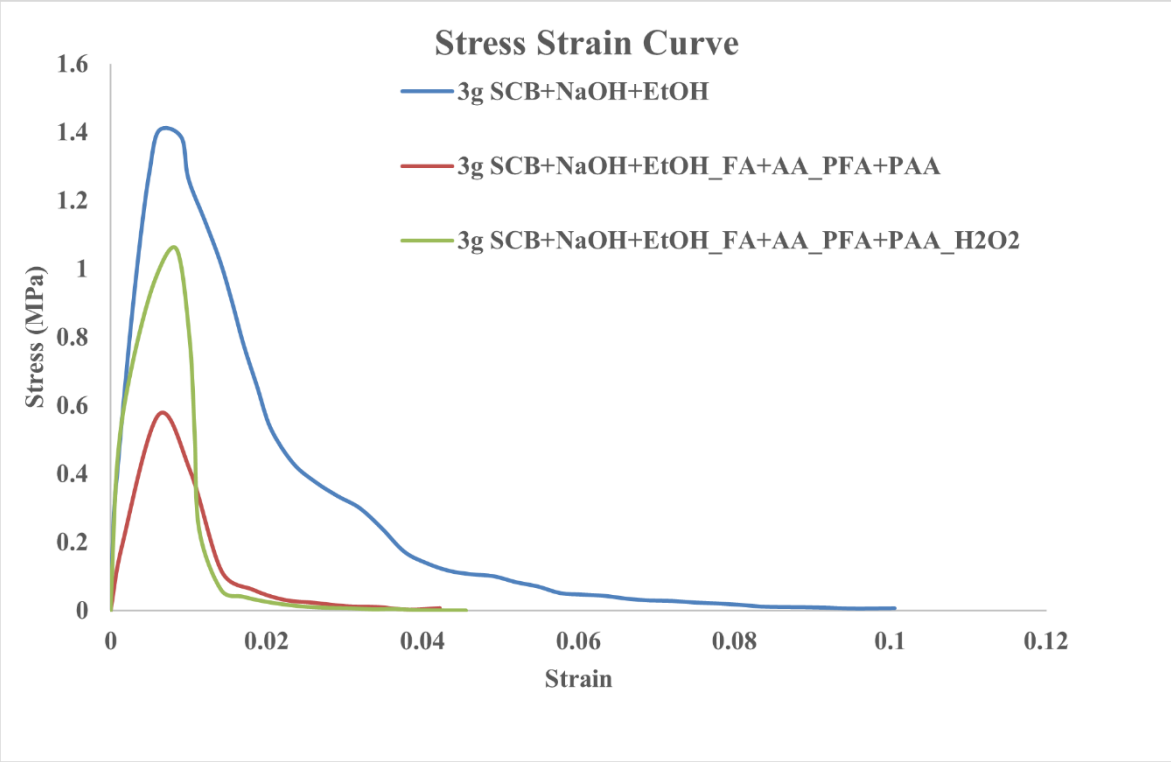

Figure 26. Stress-strain curve of membrane from 3g SCB after various treatments

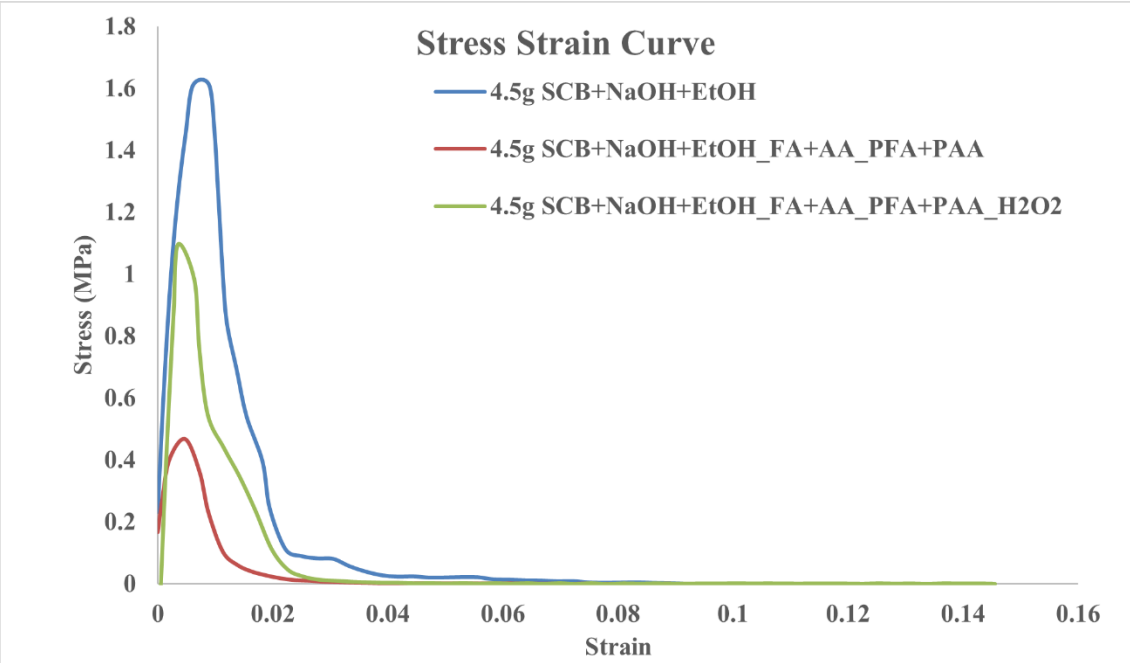

Figure 27. Stress-strain curve of membrane from 4.5g SCB after various treatments

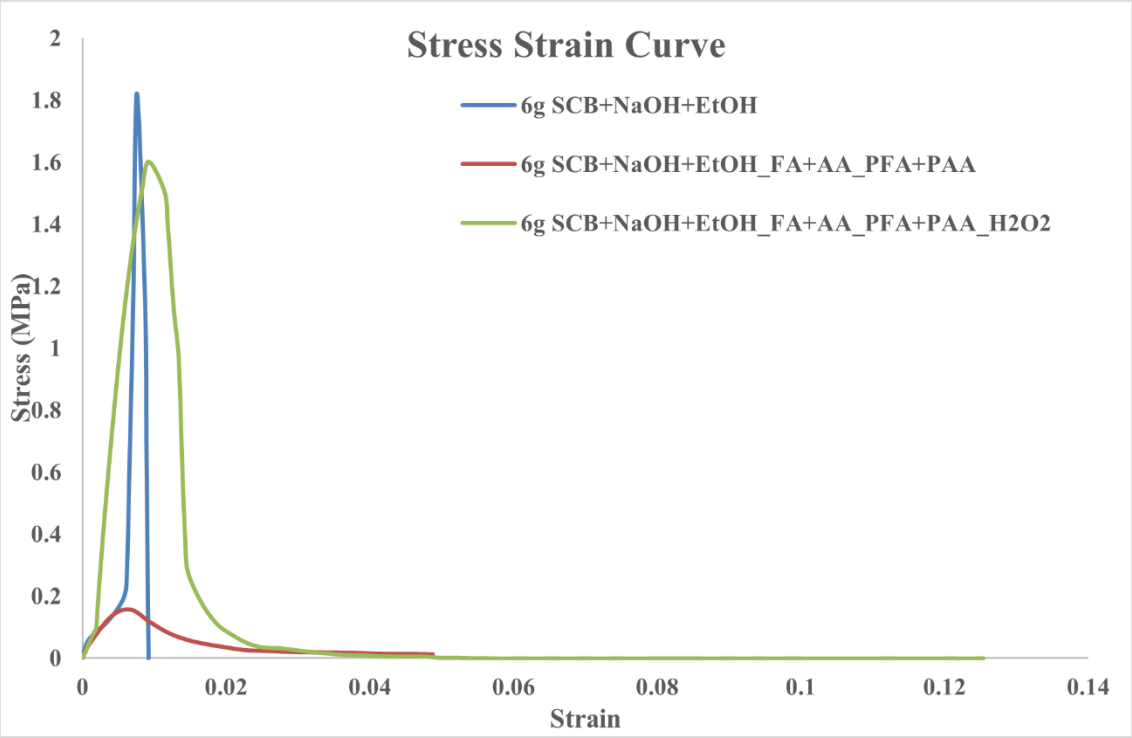

Figure 28. Stress-strain curve of membrane from 6g SCB after various treatments

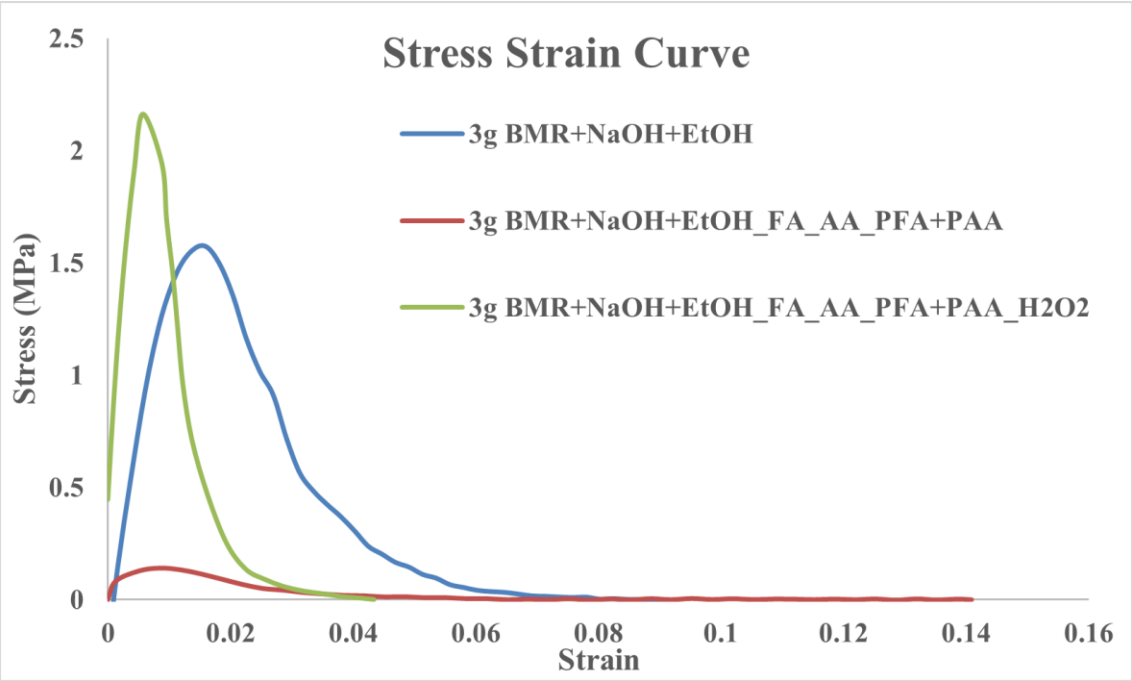

Figure 29. Stress-strain curve of membrane from 3g BMR after various treatments

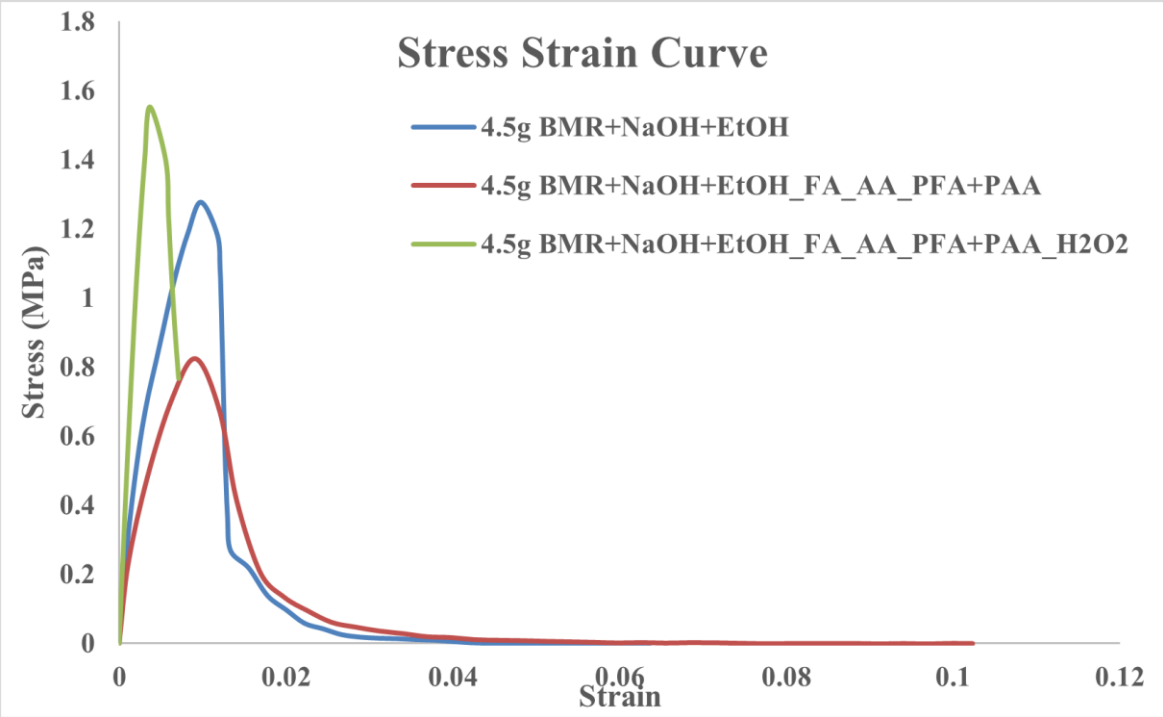

Figure 30. Stress-strain curve of membrane from 4.5g BMR after various treatments

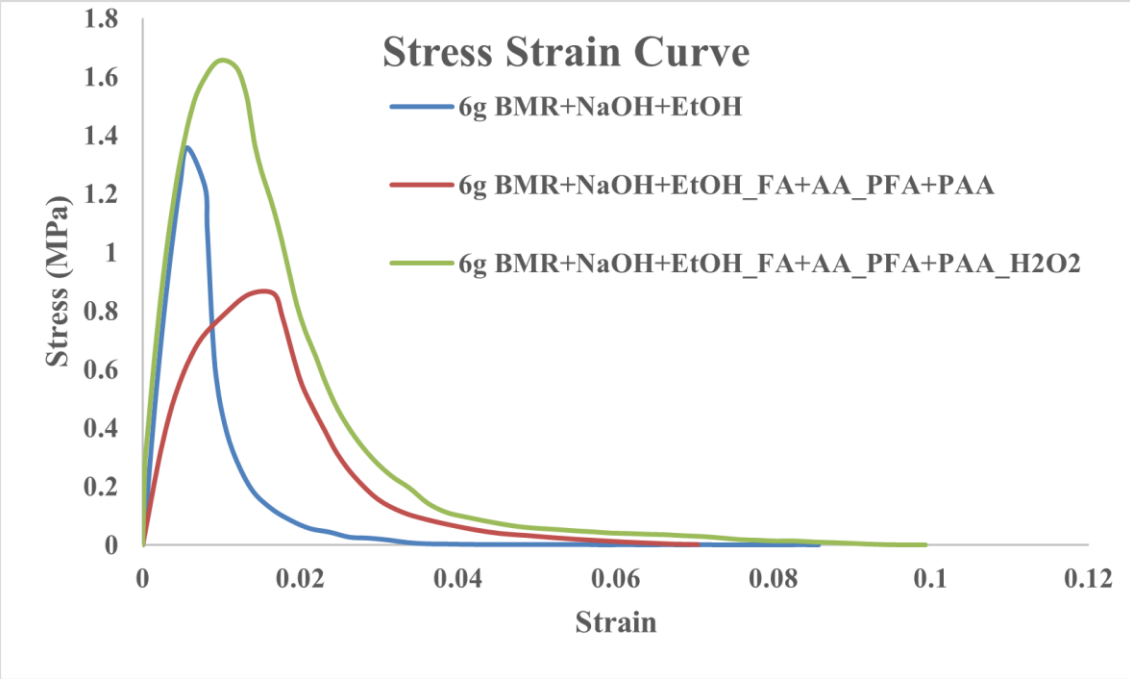

Figure 31. Stress-strain curve of membrane from 6g BMR after various treatments

4.6 Contact angle measurement

The sample was placed on the optical tensiometer table, and 6µL dosing volume was dispensed slowly on it. It was observed that the water was absorbed immediately by the membrane, indicating that the samples are very hydrophilic.

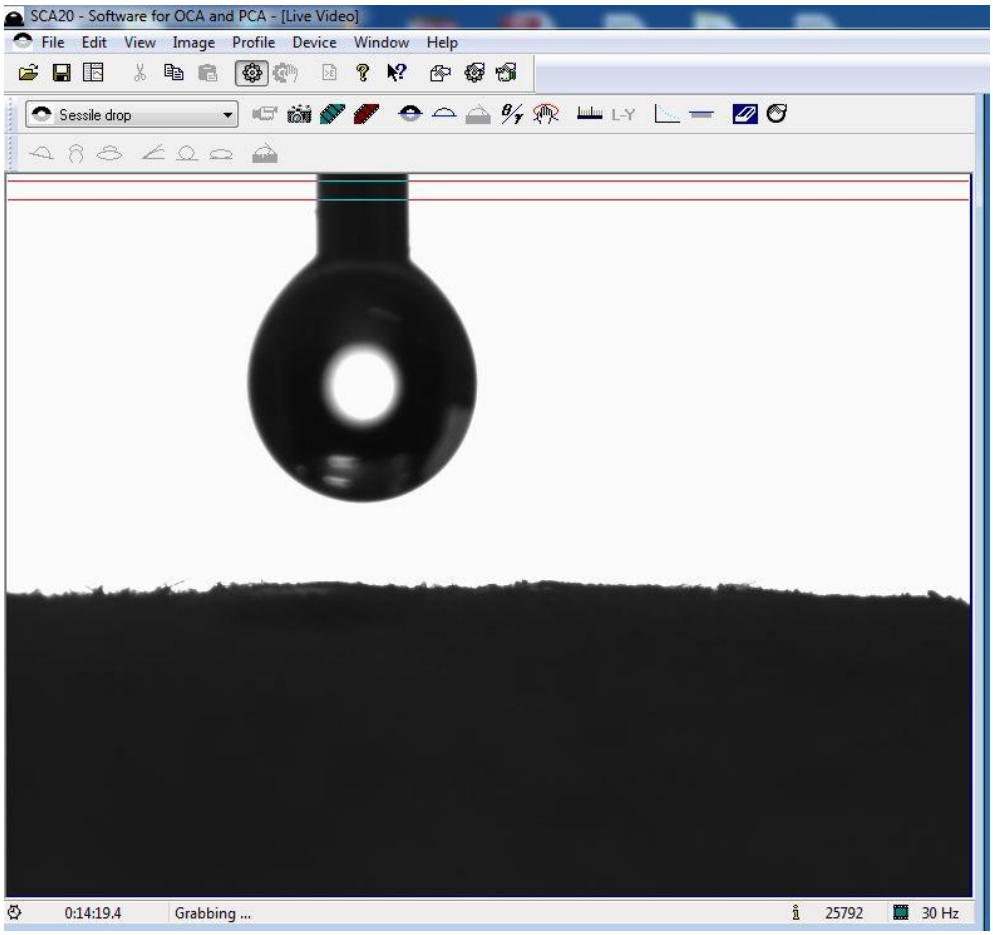

Figure 32. Dispensing liquid on the sample using optical tensiometer, as seen in SCA20 software

4.7 Particle Filtration Efficiency and Pressure drop measurement

The particle filtration efficiency of various grams of cellulose membrane extracted from SCB, and BMR was studied. The result shows that bleaching is an important factor which helps to increase filtration efficiency of the cellulose membrane.

The filtration efficiency of the bleached membrane extracted from 3 and 4.5g of SCB is 42 and 57 percent, respectively, whereas the filtration efficiency of the bleached membrane extracted from 3, 4.5, and 6g of BMR is 50, 40, and 35 percent, respectively. Filtration efficiency for the surgical facemask is 40.89 percent.

The pressure needed by a person wearing a mask to breathe through this filter membrane is known as the flow resistance. The flow resistance of the bleached membrane extracted from 3.0 and 4.5g of SCB is 68.7 and 32.8 mm.H_2O, respectively. The flow resistance of the bleached membrane from 3.0, 4.5, and 6.0g of BMR is 16.2, 38, and 51.3 mmH_2O, respectively. Surgical facemask has a flow resistance of 8.6 mm.H_2O. The outcome demonstrates the potential for using cellulose membrane from 3g SCB and BMR, 4.5g SCB and BMR, and 6g BMR as an air filter membrane.

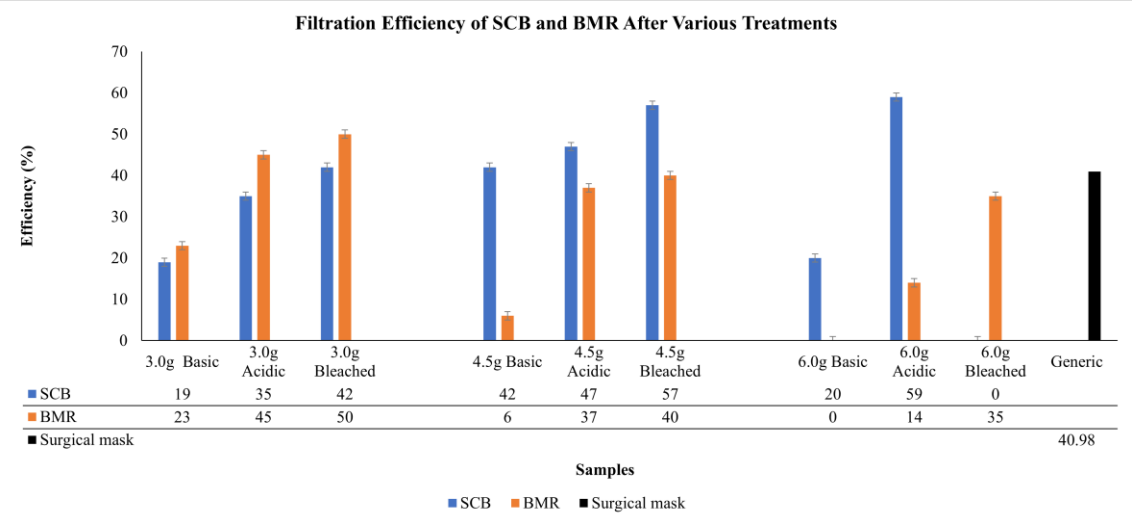

Figure 33. Filtration efficiency of SCB and BMR after various treatments

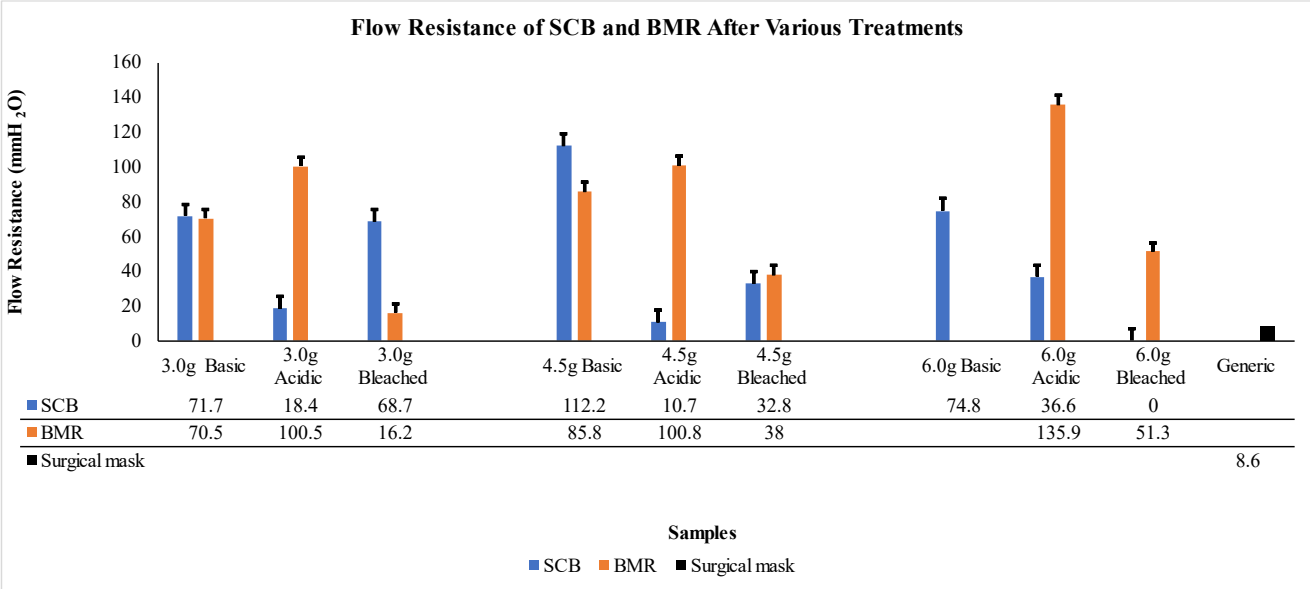

Figure 34. Flow resistance of SCB and BMR after various treatments

Note: Basic treatment means SCB/BMR treated with NaOH+EtOH

Acid treatment means SCB/BMR treated with NaOH+EtOH_FA+AA_PFA+PAA

Bleaching treatment means SCB/BMR treated with NaOH+EtOH_FA+AA_PFA+PAA _H_2O_2

4.7 Dissolution of the extracted cellulose fiber

Two techniques (vortex and freeze–thaw methods) were used to dissolve the extracted cellulose. A solution of 5ml of EDA and 1.5g of KSCN salt was vortexed until

the salt was completely dissolved. Then 0.25g of extracted cellulose was added to the vortexed solution, which was then vortexed until the cellulose was completely dissolved. The viscosity of the solution depends on the weight of cellulose added to the solution.

For the freeze thaw method, 0.25g of cellulose and 1.5g of KSCN were added to 5ml of EDA in a conical tube. The solution was set to freeze in -80 ℃ for 10 minutes, then it was dipped in a hot water bath of 40℃ until it melts. The process starting from freezing was repeated thrice. It was observed that there was no complete dissolution and a few days after dissolution, the particles coagulate again. This means that stirring is an important factor for complete dissolution of cellulose extracted from SCB and BMR in EDA and KSCN solvent.

Figure 35. Dissolution of cellulose in ethylene diamine and potassium thiocyanate via vortex method

4.7 Electrospinning

We prepared dissolved cellulose at 2.5, 4.0, 5.5, and 7.0 weight (wt) percentages for electrospinning. Due to the 2.5 wt% extremely low viscosity and the 7 wt% high viscosity (the solution was like a thick gel), the two dissolved cellulose solutions could not be electrospun. The solutions we deemed most suitable for electrospinning based on

how viscous they seemed were 4.0 and 5.5 wt%. To electrospin, various parameters such as distance between the needle and collector, flow rate, viscosity of the solution, the voltage of the machine need to be varied. Flow rate, viscosity of the solution, distance between the needle and collector, and other variables were changed during the electrospinning process, but the highest voltage we could use was 25kv. We could not achieve a good electrospinning result because of the low voltage source. According to published research[56], using a voltage source of 30–50 kV will aid in producing good electrospinning results.

4.8 Membrane biocompatibility test

The membranes extracted from SCB and BMR after basic (SCB/BMR+NaOH+EtOH), acidic (SCB/BMR+NaOH+EtOH/FA+AA/PFA+PAA) and bleaching treatments (SCB/BMR+NaOH+EtOH/FA+AA/PFA+PAA/H_2O_2)) were placed in the 24 well cell culture plate after which 70%EtOH was added to the wells. The 24 well plates were then placed under UV of the biosafety cabinet for 6 hours. After 6 hours, the EtOH is replaced and then the well plates are left under the UV overnight to sterilize the scaffolds. The scaffolds were then washed with phosphate buffer saline (PBS). In the meantime, MDA-MB-231 breast cancer cells were cultured. For seeding, 50µL volume of cells (150,000 cells total) were seeded on the cellulose membranes, and 250 µL of growth media was added until the scaffold was completely immersed. Figure 36 and 37 displays the quantitative information about cell attachment and growth on the scaffold. The growth and attachment of the cells were observed on the membrane after days 1, 2 and 3 were visualized using upright fluorescence microscope as shown in figures 38-43. The result shows that the cells were proliferating daily, and the membrane can be used as a scaffold.

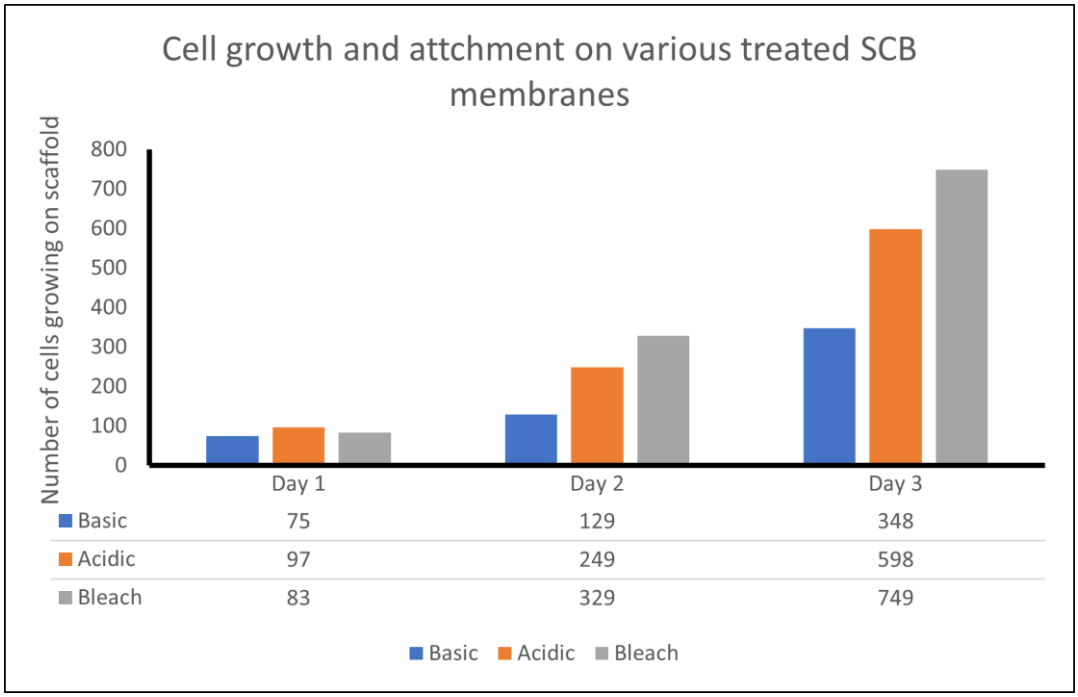

Figure 36. Cell growth and attachment on various SCB treated membrane

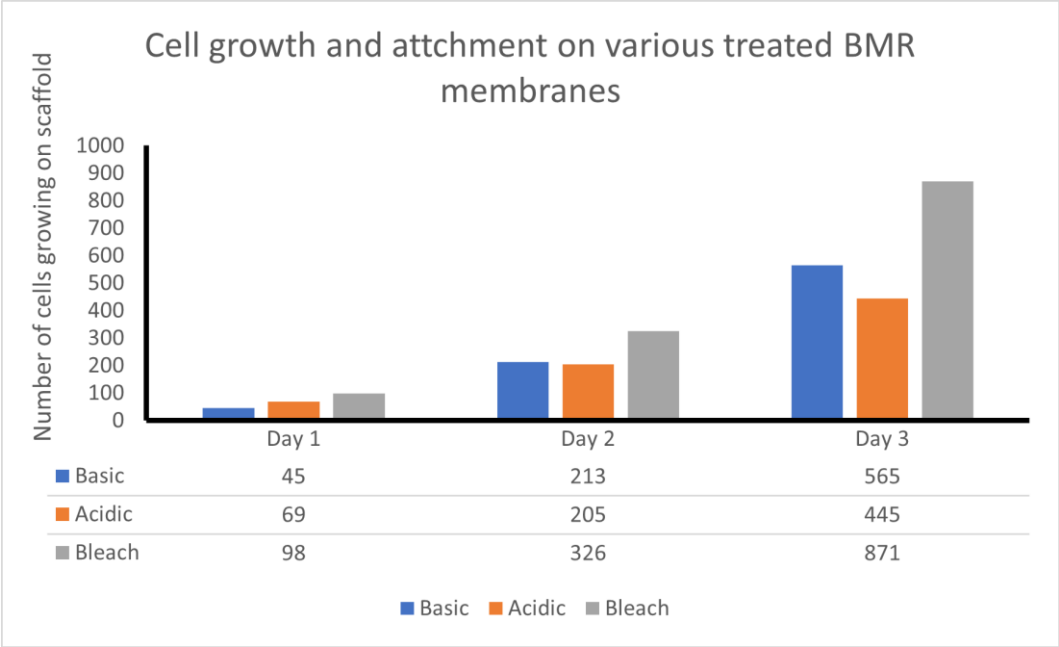

Figure 37. Cell growth and attachment on various BMR treated membrane

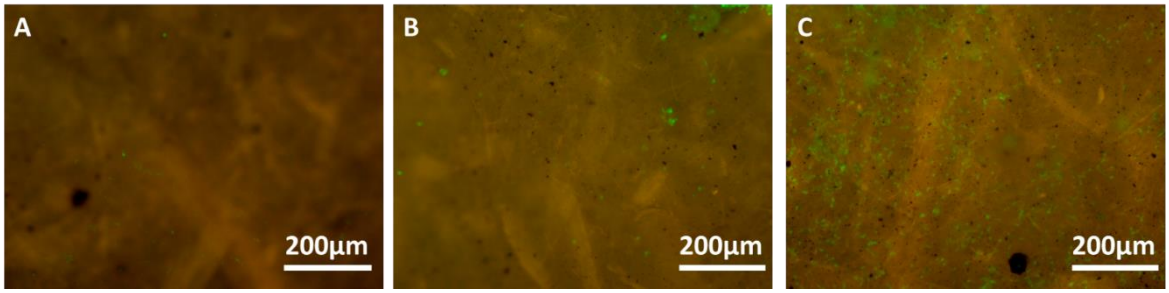

Figure 38. Cell growth and attachment of SCB after basic treatment at day: (A) 1 (B) 2 (C) 3

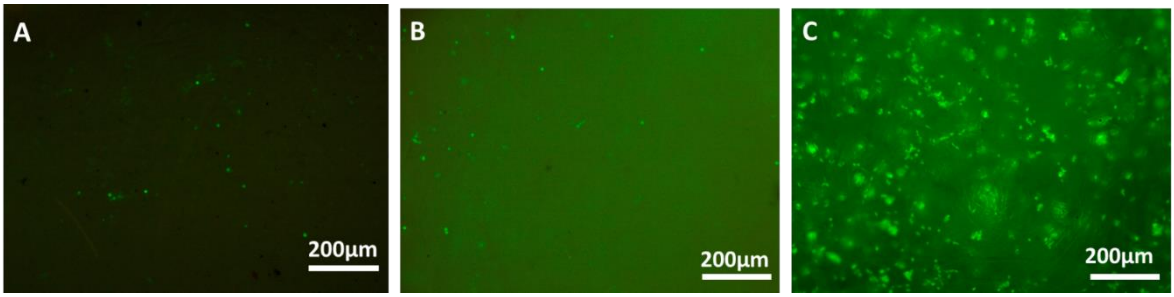

Figure 39. Cell growth and attachment of SCB after acidic treatment at day: (A) 1 (B) 2 (C) 3

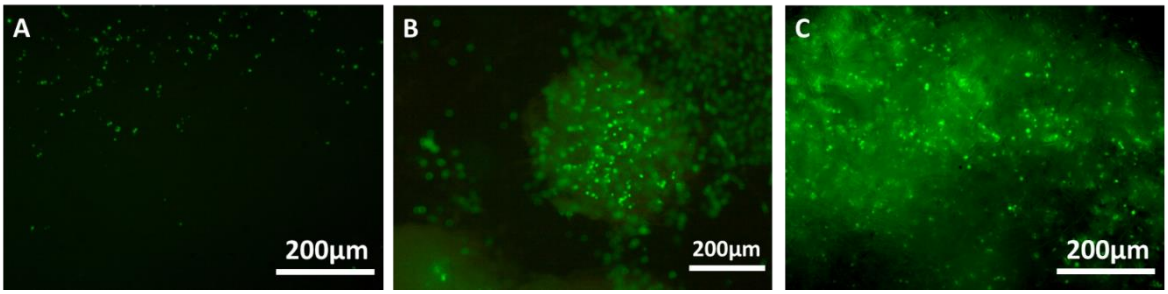

Figure 40. Cell growth and attachment of SCB after bleaching treatment at day: (A) 1 (B) 2 (C) 3

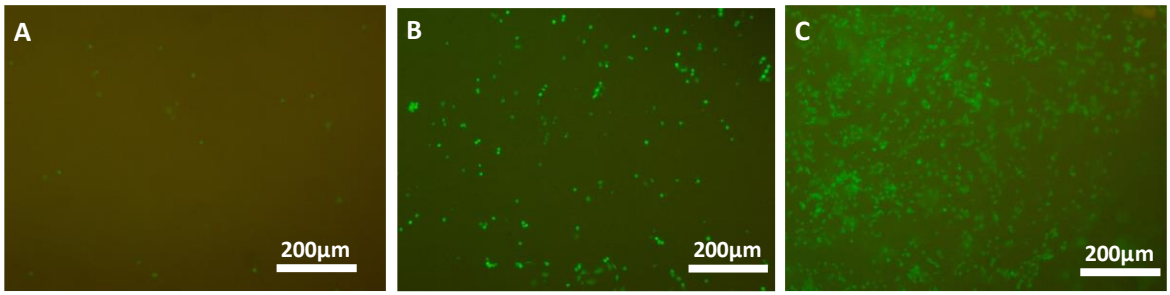

Figure 41. Cell growth and attachment of BMR after basic treatment at day: (A) 1 (B) 2 (C) 3

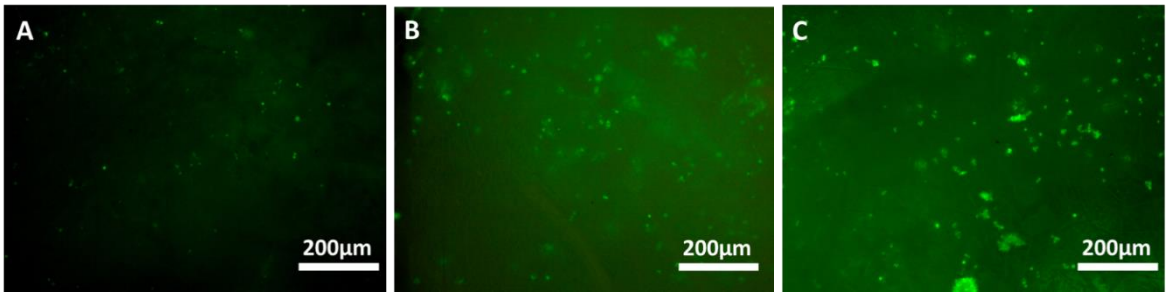

Figure 42. Cell growth and attachment of BMR after acidic treatment at day: (A) 1 (B) 2 (C) 3

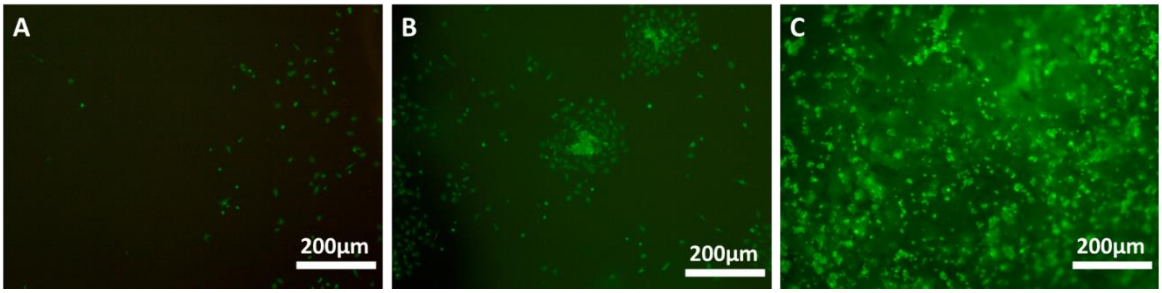

Figure 43. Cell growth and attachment of BMR after bleaching treatment at day: (A) 1 (B) 2 (C) 3

CHAPTER 5

CONCLUSION and RECOMMENDATIONS

5.1 Conclusion

The extraction of cellulose from sugarcane bagasse and banana mid rib is an environmentally friendly process and the use of these two raw materials (SCB and BMR) will contribute to environmental sustainability and improve the quality of life through reduction in environmental pollution caused by these waste materials. The functional groups of the bleached post-treated material extracted from SCB and BMR revealed that the extracted material is cellulose. This was further proved through thermogravimetric analysis, which revealed that the decomposition temperature of post-treated material aligns with cellulose. The bleached hydrophilic cellulose membrane extracted from 3 and 4.5g SCB and BMR can be used effectively as an air filter membrane for face mask. Finally, the membrane can be used as scaffold for tissue engineering application.

5.2 Recommendations

We have been able to dissolve the extracted cellulose using ethylene diamine and potassium thiocyanate and prove that vortex method is the most efficient method for dissolving. One of the challenges we faced with electrospinning was inability to use voltage above 20KV. Future work needs to be done on electrospinning by using a high voltage source device or another solvent to obtain uniform network on interconnected fibers and this might also improve the mechanical strength of the filter. The exterior part of the filter needs to be treated to make it hydrophobic so as to repel water penetration.

Furthermore, quantitative analysis needs to be done on the scaffold to have detailed information about the ratio of live to dead cells, and also to know the most effective membrane and treatment required to obtain efficient scaffolds.

REFERENCES

1. Mukherjee, S., et al., *PVA-graphene-hydroxyapatite electrospun fibres as air-filters.* Materials Research Express, 2020. **6**(12).
2. Konda, A., et al., *Aerosol Filtration Efficiency of Common Fabrics Used in Respiratory Cloth Masks.* ACS Nano, 2020. **14**(5): p. 6339-6347.
3. Boix Rodríguez, N., et al., *Engineering Design Process of Face Masks Based on Circularity and Life Cycle Assessment in the Constraint of the COVID-19 Pandemic.* Sustainability, 2021. **13**(9).
4. Dugdale, C.M. and R.P. Walensky, *Filtration Efficiency, Effectiveness, and Availability of N95 Face Masks for COVID-19 Prevention.* JAMA Internal Medicine, 2020. **180**(12): p. 1612-1613.
5. Denmark, U.o.S. *Face masks and the environment: Preventing the next plastic problem*. (2021, March 10) [cited 2022 Retrieved March 31]; Available from: www.sciencedaily.com/releases/2021/03/210310122431.htm.
6. Xu, E.G. and Z.J. Ren, *Preventing masks from becoming the next plastic problem.* Frontiers of Environmental Science & Engineering, 2021. **15**(6): p. 125.
7. Tabatabaei, M., et al., *Exergy intensity and environmental consequences of the medical face masks curtailing the COVID-19 pandemic: Malign bodyguard?* Journal of cleaner production, 2021. **313**: p. 127880-127880.
8. Zheng, J. and S. Suh, *Strategies to reduce the global carbon footprint of plastics.* Nature Climate Change, 2019. **9**(5): p. 374-378.
9. Jung, S., et al., *Valorization of disposable COVID-19 mask through the thermo-chemical process.* Chemical Engineering Journal, 2021. **405**: p. 126658.
10. Johar, N., I. Ahmad, and A. Dufresne, *Extraction, preparation and characterization of cellulose fibres and nanocrystals from rice husk.* Industrial Crops and Products, 2012. **37**(1): p. 93-99.
11. Canché-Escamilla, G., et al., *Production of cellulose from banana plant agricultural waste.* 2005. **16**: p. 83-88.
12. Araldi da Silva, B., et al., *Electrospinning of cellulose using ionic liquids: An overview on processing and applications.* European Polymer Journal, 2021. **147**.
13. Kalia, S., et al., *Cellulose-Based Bio- and Nanocomposites: A Review.* International Journal of Polymer Science, 2011. **2011**: p. 1-35.
14. Paulo Henrique Fernandes Pereira, H.C.J.V., Maria Odila Hilário Cioffi, Daniella Regina Mullinari, Sandra Maria Da Luz, Maria Lucia Caetano Pinto Da Silva, *SUGARCANE BAGASSE PULPING AND BLEACHING: THERMAL AND CHEMICAL CHARACTERIZATION.* BioResources, 2011.
15. Reddy, N. and Y. Yang, *Fibers from Banana Pseudo-Stems*, in *Innovative Biofibers from Renewable Resources*, N. Reddy and Y. Yang, Editors. 2015, Springer Berlin Heidelberg: Berlin, Heidelberg. p. 25-27.
16. Nguyen, S.T., et al., *Cellulose Aerogel from Paper Waste for Crude Oil Spill Cleaning.* Industrial & Engineering Chemistry Research, 2013. **52**(51): p. 18386-18391.
17. He, Z., et al., *Fabrication of new cellulose acetate blend imprinted membrane assisted with ionic liquid ([BMIM]Cl) for selective adsorption of salicylic acid from industrial wastewater.* Separation and Purification Technology, 2015. **145**: p. 63-74.
18. Nataraj, S.K., et al., *Cellulose acetate-coated α-alumina ceramic composite tubular membranes for wastewater treatment.* Desalination, 2011. **281**: p. 348-353.
19. Rahman, M.Z., et al., *Face Masks to Combat Coronavirus (COVID-19)—Processing, Roles, Requirements, Efficacy, Risk and Sustainability.* Polymers, 2022. **14**.

20. Mukherjee, S., et al., *PVA-graphene-hydroxyapatite electrospun fibres as air-filters.* Materials Research Express, 2020. **6**(12): p. 125366.
21. Wang, S., et al., *Electret Polyvinylidene Fluoride Nanofibers Hybridized by Polytetrafluoroethylene Nanoparticles for High-Efficiency Air Filtration.* ACS Applied Materials & Interfaces, 2016. **8**(36): p. 23985-23994.
22. Desai, K., et al., *Nanofibrous chitosan non-wovens for filtration applications.* Polymer, 2009. **50**(15): p. 3661-3669.
23. Cauchie, H.-M., *Chitin production by arthropods in the hydrosphere.* Hydrobiologia, 2002. **470**: p. 63-95.
24. Obi Reddy, K., C. Maheswari, and D.M. Shukla, *Physico-Chemical Characterization of Cellulose Extracted from Ficus Leaves.* Journal of Biobased Materials and Bioenergy, 2013. **7**: p. 496-499.
25. Ranganagowda, R.P.G., S.S. Kamath, and B. Bennehalli, *Extraction and Characterization of Cellulose from Natural Areca Fiber.* Material Science Research India, 2019. **16**(1): p. 86-93.
26. Zhang, X., et al., *Biomimetic Supertough and Strong Biodegradable Polymeric Materials with Improved Thermal Properties and Excellent UV-Blocking Performance.* Advanced Functional Materials, 2019. **29**(4).
27. Li, R.J., et al., *A lignin-epoxy resin derived from biomass as an alternative to formaldehyde-based wood adhesives.* Green Chemistry, 2018. **20**(7): p. 1459-1466.
28. Qian, Y., X. Qiu, and S. Zhu, *Lignin: A nature-inspired sun blocker for broadspectrum Sunscreens.* Green Chemistry, 2015. **17**(1): p. 320-324.
29. Wang, S., et al., *From tree to tape: direct synthesis of pressure sensitive adhesives from depolymerized raw lignocellulosic biomass.* ACS central science, 2018. **4**(6): p. 701-708.s
30. li, R., et al., *Dissolution of cellulose from different sources in an NaOH/urea aqueous system at low temperature.* Cellulose, 2015. **22**.
31. Frey, M.W., et al., *Dissolution of cellulose in ethylene diamine/salt solvent systems.* Cellulose, 2006. **13**(2): p. 147-155.
32. Rosenau, T., et al., *Cellulose solutions in N-methylmorpholine-N-oxide (NMMO) – degradation processes and stabilizers.* Cellulose, 2002. **9**: p. 283-291.
33. Reddy, N. and Y. Yiqi, *The N-Methylmorpholine-N-Oxide (NMMO) Process of Producing Regenerated Fibers*. 2015. p. 65-71.
34. Rosenau, T. and A. French, *N-Methylmorpholine-N-oxide (NMMO): hazards in practice and pitfalls in theory.* Cellulose, 2021. **28**.
35. Fink, H.-P., Weigel, P., Purz, H.J., and Ganster, J., *Structure formation of regenerated cellulose materials from NMMO-solutions.* Elsevier, 2001.
36. Yuan, H., et al., *Ultra-high-strength composite films prepared from NMMO solutions of bamboo-derived dissolving pulp and chitosan.* Industrial Crops and Products, 2021. **170**: p. 113747.
37. Borbély, É., *Lyocell, The New Generation of Regenerated*

Cellulose. Acta Polytechnica Hungarica, 2008. **5**(3): p. 8.
38. Sayyed, A.J., et al., *Structural characterization of cellulose pulp in aqueous NMMO solution under the process conditions of lyocell slurry.* Carbohydrate Polymers, 2019. **206**: p. 220-228.
39. Ciacco, G.T., et al., *Application of the solvent dimethyl sulfoxide/tetrabutyl-ammonium fluoride trihydrate as reaction medium for the homogeneous acylation of Sisal cellulose.* Cellulose, 2003. **10**(2): p. 125-132.

40. Ramos, L.A., E. Frollini, and T. Heinze, *Carboxymethylation of cellulose in the new solvent dimethyl sulfoxide/tetrabutylammonium fluoride.* Carbohydrate Polymers, 2005. **60**: p. 259-267.
41. Swatloski, R.P., et al., *Dissolution of Cellose with Ionic Liquids.* Journal of the American Chemical Society, 2002. **124**(18): p. 4974-4975.
42. Sadat-Shojai, M., et al., *Electrospinning of liquefied banana stem residue in conjugation with hydroxyapatite nanocrystals: towards new scaffolds for bone tissue engineering.* Cellulose, 2022.
43. Turnbull, G., et al., *3D bioactive composite scaffolds for bone tissue engineering.* Bioactive Materials, 2018. **3**(3): p. 278-314.
44. Meng, F., et al., *Extraction and characterization of cellulose nanofibers and nanocrystals from liquefied banana pseudo-stem residue.* Composites Part B: Engineering, 2019. **160**: p. 341-347.
45. López, S.E. and J. Salazar, *Trifluoroacetic acid: Uses and recent applications in organic synthesis.* Journal of Fluorine Chemistry, 2013. **156**: p. 73-100.
46. Guedes, W.N. and F.M.V. Pereira, *Classifying impurity ranges in raw sugarcane using laser-induced breakdown spectroscopy (LIBS) and sum fusion across a tuning parameter window.* Microchemical Journal, 2018. **143**: p. 331-336.
47. Aye, T., T. Nu, and C. Cho, *STUDIES ON SOME PHYSICOMECHANICAL AND ANTIMICROBIAL PROPERTIES OF PREPARED CELLULOSE HYDROGEL FILMS.* 2019.
48. Jayaprabha, J., M. Brahmakumar, and M. Vattackatt, *Banana Pseudostem Characterization and Its Fiber Property Evaluation on Physical and Bioextraction.* Journal of Natural Fibers, 2011. **8**: p. 149-160.
49. Oliveira, L., et al., *Chemical composition of different morphological parts from 'Dwarf Cavendish' banana plant and their potential as a non-wood renewable source of natural product.* Industrial Crops and Products, 2007. **26**: p. 163.
50. Bogart, J. *Moisture Content vs Water Activity*. 2018 [cited 2018 April 26]; Available from: https://blog.kett.com/bid/362219/moisture-content-vs-water-activity-use-both-to-optimize-food-safety-and-quality.
51. Karppinen, A. *TEMPERATURE STABILITY OF CELLULOSE FIBRILS*. 2018 [cited 2022 July 6]; Available from: https://blog.borregaard.com/exilva/temperature-stability-of-cellulose-fibrils#:~:text=Temperature%20stability%20at%20dry%20state&text=These%20components%20have%20different%20decomposition,they%20degrade%20at%20higher%20temperature.
52. Yeap, S.P., *Utilization of Palm Pressed Pericarp Fiber: Pretreatment, Optimization, and Characterization.* Environmental Progress & Sustainable Energy, 2013.
53. Liu, S., et al., *Cellulose acetate nanofibers with photochromic property: Fabrication and characterization.* Materials Letters - MATER LETT, 2010. **64**: p. 2427-2430.
54. Arumugam, M., et al., *Electrospinning cellulose acetate/silk fibroin/Au-Ag hybrid composite nanofiber for enhanced biocidal activity against MCF-7 breast cancer cell.* Materials Science and Engineering: C, 2021. **123**: p. 112019.
55. Paar, A. *Capillary flow porometry basics: measuring through pores*. 2020 [cited 2022 July 1]; Available from: https://wiki.anton-paar.com/en/basics-of-capillary-flow-porometry/.
56. Joo, M.W.F.a.Y.L. *CELLULOSE SOLUTION IN NOVEL SOLVENT AND ELECTROSPINNING THEREOF*. 2004 [cited 2022 July 13]; Patent:[Available from: https://patents.google.com/patent/US20050247236A1/en.